

FILE COPY

4

AD-A215 118

Technical Document 1606
June 1989

Neurobeamformer II: Further Exploration of Adaptive Beamforming via Neural Networks

S. L. Speidel

DTIC
ELECTE
NOV 22 1989
S B D

Approved for public release; distribution is unlimited.

*Original contains color
plates: All DTIC reproductions
will be in black and
white*

89 11 21 041

NAVAL OCEAN SYSTEMS CENTER
San Diego, California 92152-5000

E. G. SCHWEIZER, CAPT, USN
Commander

R. M. HILLYER
Technical Director

ADMINISTRATIVE INFORMATION

This work was performed during the period October 1987-September 1988 for the Chief of Naval Research, Independent Exploratory Development Programs (IED), OCNR-201, Arlington, VA 22217, under program element 0602936N.

Released by
M. B. Klausen, Head
Analysis Branch

Under authority of
R. H. Moore, Head
ASW Technology
Division

ACKNOWLEDGMENT

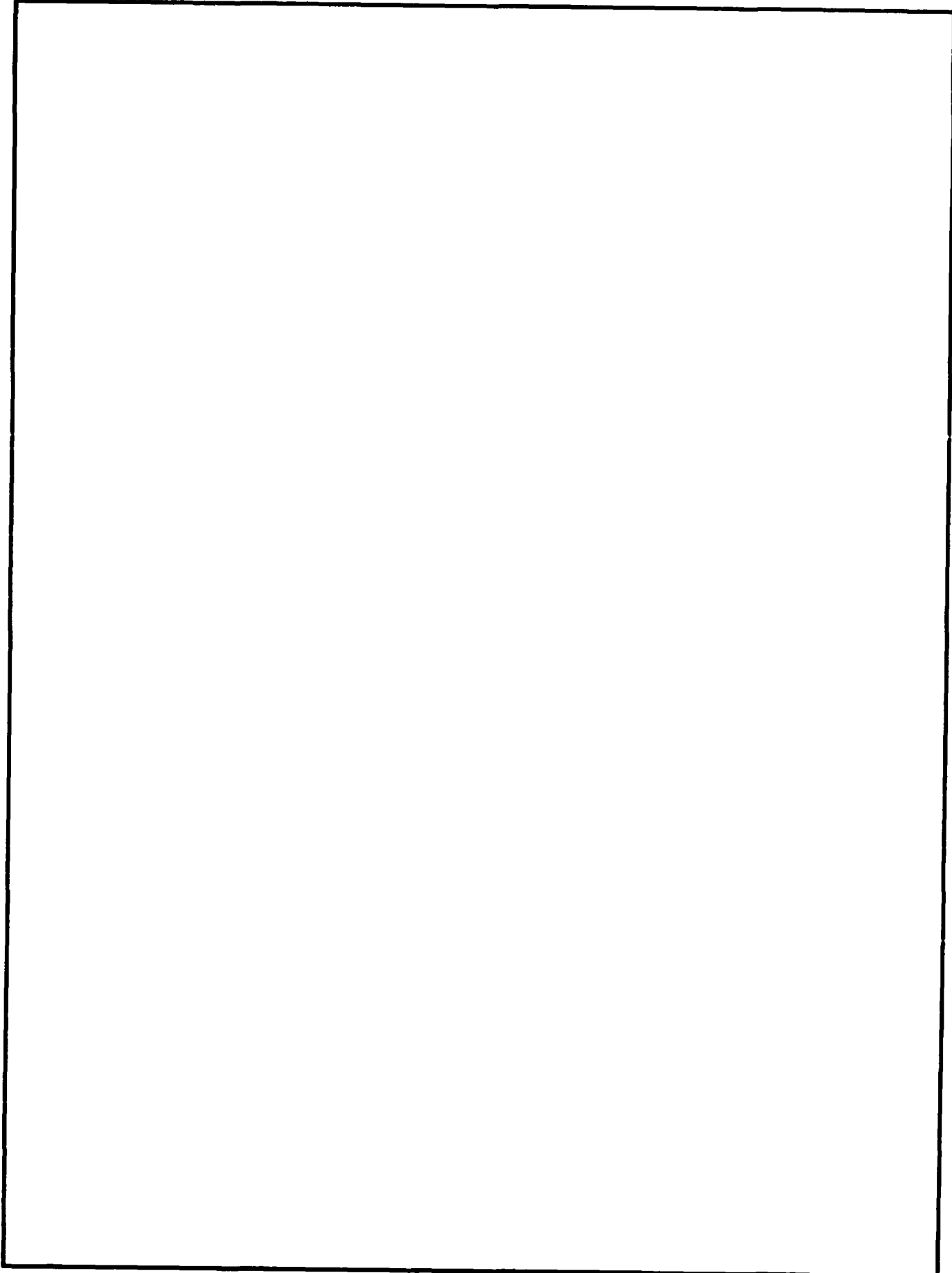
The author wishes to thank Dr. John Silva, Program Director for Technology; his associates, Dr. Kenneth J. Campbell and Mr. Robert E. Munn, NOSC Code 014, for the support.

REPORT DOCUMENTATION PAGE

1a. REPORT SECURITY CLASSIFICATION UNCLASSIFIED		1b. RESTRICTIVE MARKINGS	
2a. SECURITY CLASSIFICATION AUTHORITY		3. DISTRIBUTION/AVAILABILITY OF REPORT Approved for public release; distribution is unlimited.	
2b. DECLASSIFICATION/DOWNGRADING SCHEDULE			
4. PERFORMING ORGANIZATION REPORT NUMBER(S) NOSC TD 1606		5. MONITORING ORGANIZATION REPORT NUMBER(S)	
6a. NAME OF PERFORMING ORGANIZATION Naval Ocean Systems Center	6b. OFFICE SYMBOL (if applicable) Code 632	7a. NAME OF MONITORING ORGANIZATION	
6c. ADDRESS (City, State and ZIP Code) Analysis Branch ASW Technology Division San Diego, CA 92152-5000		7b. ADDRESS (City, State and ZIP Code)	
8a. NAME OF FUNDING/SPONSORING ORGANIZATION Chief of Naval Research	8b. OFFICE SYMBOL (if applicable) OCNR-201	9. PROCUREMENT INSTRUMENT IDENTIFICATION NUMBER	
8c. ADDRESS (City, State and ZIP Code) Independent Exploratory Development Programs Arlington, VA 22217		10. SOURCE OF FUNDING NUMBERS	
		PROGRAM ELEMENT NO. 0602936N	AGENCY ACCESSION NO. DN308 120
		PROJECT NO. RV36121	TASK NO. 632-ZE73
11. TITLE (include Security Classification) NEUROBEAMFORMER II: Further Exploration of Adaptive Beamforming via Neural Networks			
12. PERSONAL AUTHOR(S) S. L. Speidel			
13a. TYPE OF REPORT Final	13b. TIME COVERED FROM Oct 1987 TO Sep 1988	14. DATE OF REPORT (Year, Month, Day) June 1989	15. PAGE COUNT 54
16. SUPPLEMENTARY NOTATION			
17. COSATI CODES		18. SUBJECT TERMS (Continue on reverse if necessary and identify by block number)	
FIELD	GROUP	SUB-GROUP	
			neuroprocessor technology cross-correlation target locator
			neurobeamformer, artificial neural networks long-term potentiation standard echo generator
			neural network auditory target strength standardization program
19. ABSTRACT (Continue on reverse if necessary and identify by block number)			
<p>This paper discusses neural network technology as a tool for signal processing. Test results show that the adaptive beamformer method, based on neural network technology, performs the desired function of directing a beam so as to enhance a target signal and reject noise and interference. Comparing test output values with a matched-correlation output, we noted that the plotted crossbar circuit energy minima follow the shape of an inverted match-filter output.</p> <p>The neurobeamformer has certain advantages of implementation and adaptability over other methods. In concept, it is implementable in analog circuitry with no control code required. Thus a compact, simple, low-cost processor component that is not sensitive to array grooming can be produced.</p> <p>We realize that a straightforward adaptive beamformer cannot match the interference-cancellation performance of more exotic methods, which include sidelobe cancellers. So, a neuroprocessor, that will include a neurobeamformer as a component, will be built. This neuroprocessor will provide for cancellation of sidelobes, enhance source discrimination and angle-estimation through interaction of beams. Plans for this extended network were influenced by studies of the literature in biological sensory processing, both peripheral and central.</p>			
20. DISTRIBUTION/AVAILABILITY OF ABSTRACT <input type="checkbox"/> UNCLASSIFIED/UNLIMITED <input checked="" type="checkbox"/> SAME AS RPT <input type="checkbox"/> DTIC USERS		21. ABSTRACT SECURITY CLASSIFICATION UNCLASSIFIED	
22a. NAME OF RESPONSIBLE PERSON S. L. Speidel		22b. TELEPHONE (Include Area Code) (619) 553-1557	22c. OFFICE SYMBOL Code 632

UNCLASSIFIED

SECURITY CLASSIFICATION OF THIS PAGE (When Data Entered)



CONTENTS

1.	INTRODUCTION	1
2.	BACKGROUND	1
3.	CROSSBAR BEAMFORMING METHOD	3
	3.1 Basic Components And Their Functions	3
	3.2 Discussion	4
	3.3 Network Controlled Combiner Theory	4
4.	ASSOCIATED NEUROMORPHOLOGY	7
	4.1 General Organizational Trends in Biological Sensory Systems	7
	4.2 Auditory Cross-Correlation Models	7
5.	SUGGESTED EXTENSIONS	8
	5.1 A Demonstrator	8
	5.2 Neuroprocessor	8
	5.3 Target Locator	10
6.	DISCUSSION OF TEST RESULTS	11
	6.1 The Simulator	11
	6.2 The Data	11
	6.3 The Results	12
	6.4 Example Test Outputs	13
7.	GENERAL CONSIDERATIONS AND CAPABILITIES	56
	7.1 Overview	56
	7.2 Applications	56
	7.2.1 Guiding Weapons to their Mission Targets	56
	7.2.2 Maneuvering Among Obstacles or Landmarks	57
	7.2.3 Image Processing	57
	7.2.4 General Least Square Parameter Estimation	57
8.	REFERENCES	58
9.	GLOSSARY	59
	APPENDIX A — Connection Strength Plots, Point Target, SIR = 0dB (Iteration \approx 0.8 ms)	A-1

FIGURES

1.	Adaptive beamformer	4
2.	Hopfield crossbar circuit	6
3.	Response areas of single neurons of the peripheral auditory system of the cat	9
4.	Venn diagram of beam patterns	9

	For
xI	<input checked="" type="checkbox"/>
ed	<input type="checkbox"/>
lon/	<input type="checkbox"/>
ility Codes	
Dist	Avail and/or Special
A-1	

FIGURES (cont.)

5.	Overview plan for the target locator	10
6.	Lateral interaction technique for target locator	11
7.	The testing system	12
8.	Spectrograms of down-translated signals: (a) Interference only, (b) target only, speed = 15 knots, (c) target & interference, SIR = 0 dB	15
9.	Sensitivity and crossbar energy histories for case of no target, interference only	17
10.	Sensitivity and crossbar energy histories for case of point target, SIR = -30 dB, speed = 15 knots; interference same as figure 9	19
11.	Spectrograms of down-translated signals: (a) interferences only, (b) target only, speed = 0 knot, (c) target & interference, SIR = 0 dB	21
12.	Sensitivity history for point target at SIR = 0 dB, speed = 0 knot	25
13.	Crossbar network energy history for point target at SIR = 0 dB, speed = 0 knot	27
14.	(a) Beam output and sensor input for channel 1, for same case as figures 12 and 13. (b) Matched-filter/cross-correlation results	28
15.	Snapshots of evolving/adapting beam: (a) before target echo return (b) after target echo return. Red is high energy, blue is low energy	29
16.	Connectivity histories for case of point target and SIR = 0 dB (Iteration \approx 0.8 ms)	31
17.	Input current histories for point target, SIR = 0 dB (Iteration \approx 0.8 ms)	33
18.	Input currents (continued from figure 17. Iteration \approx 0.8 ms)	34
19.	Connection strength and input current value ranges for case of point target and SIR = 0 dB	35
20.	Sensitivity history for case: point target, SIR = -15 dB, speed = 0 knot	37
21.	Crossbar network energy history for case: point target, SIR = -15 dB, speed = 0 knot	39
22.	Snapshots of evolving/adapting beams on polar scale for: (a) before target echo return, (b) after target echo return. Beam is yellow because the SIR is -15 dB and the energy does not go as low as for the case, SIR = 0 dB. Target is at 26 degrees	41
23.	(a) Beam output and input stream for channel 1. (b) Matched-filter/cross-correlation values	43
24.	Connectivity histories for the case: point target, SIR = -dB, speed = 0 knot. (Iteration = 0.8 ms)	45
25.	Sensitivity history for case: distributed target, SIR = 0 dB, speed = 0 knot	47
26.	Crossbar network energy history for case: distributed target, SIR = 0, speed = 0 knot	49
27.	Snapshots of evolving/adapting beam on a polar scale for case: distributed target, SIR = 0 dB, speed = 0 knot	51
28.	Connection strength histories for case: distributed target, SIR = 0 dB, speed = 0 knot. (Iteration = 0.8 ms)	53
29.	(a) Beam output and input stream for channel 1, (b) Matched-filter cross-correlation values case: distributed target, SIR = 0 dB, speed = 0 knot	55

1. INTRODUCTION

Tests show that the adaptive beamformer method, based on neural network technology, performs the desired function of directing a beam so as to enhance a target signal and reject noise and interference. The interference-rejection performance of the method has not yet been quantitatively compared with other methods, but it is clear from the tests reported here that the beamformer is performing as expected. It has been noted, from comparison of the test output values and a matched-correlator output, that the plotted crossbar circuit energy function minima follow the shape of an inverted matched-filter output. This makes sense if we look at how the connectivities and the currents are computed from the signal, and their role in the energy equation.

The neurobeamformer has certain advantages of implementation and adaptability over other methods. It is, in concept at least, implementable in analog circuitry with no control code required. This allows a compact, simple, low-cost processor component to be produced. Also, the method is not sensitive to array grooming as are some of the alternate techniques.

When tested with available recordings from an undersea array and synthesized target echoes, the beamformer points a beam, of width and character determined by the array spacing and aperture, directly at the target and leaves it there for a period of time approximately equal to twice the duration of the target echo. It does so for signal-to-interference ratios (SIRs) as low as -15 decibels (ratio of mean square amplitudes in the time domain, during the time of the target echo). Below this value there are problems discriminating the target from the interference in the case where the target echo spectrum is overlapped by the interference spectrum. This overlap happens, for example, when the target is stationary. In the case where the target is in motion with respect to the medium (approximately 15 knots in the general direction of the receiver), the beamformer performs well down to an SIR of -30 decibels.

It is recognized that a straightforward adaptive beamformer cannot match the interference-cancellation performance of more exotic methods, which include sidelobe cancellers, etc.^{1,2,3} Therefore, a neuroprocessor will be constructed which incorporates the neurobeamformer as a component, and will provide for cancellation of sidelobes, enhanced source discrimination, and angle estimation through interaction of beams. Plans for this extended network were influenced by studies of the literature in biological sensory processing, peripheral and central.

2. BACKGROUND

This report is mainly about the use of particular neural network techniques as tools for signal processing, but it is appropriate that some discussion of the neural network approach be inserted at this point, before getting to specific cases.

The computational neuroscience discipline stems from a recognition that the experimental techniques and theoretical explanations of the neurobiological sciences have progressed to the point where they will produce contributions to the hard computational disciplines. Artificial neural networks (ANNs) are the models/tools which have been forged by this discipline, for the purpose of engineering devices. If our devices can accomplish what biological neural tissue accomplishes in the areas of information processing and control, while retaining the advantages of our conventional computing machines, then certain areas of application will benefit greatly.

Two areas which will benefit are (1) unmanned space exploration and (2) defense (weapons). Both have the need for powerful information processing under conditions that are adverse to humans and other biological systems. Except for the adverse conditions (no air, small platforms, exploding warheads) an option would be to improve the interface between man and machine, perhaps forming a direct interface between the brain and the computer i.e., putting machines into man. But this combination does not work for autonomous weapons and spacecraft because it retains the weight, size, environmental requirements, and vulnerabilities of the biological system. Thus the alternate approach of putting man (or elements of man) into machines, so to speak, is preferable.

In general, the role of ANNs in the applications arena will be that of tools residing in the engineer's tool box, to be applied whenever the tools fit. The following items should be held to be distinct from one another: (1) what can be accomplished by using the ANNs which are presently defined and (2) what can be accomplished eventually through the ANNs which will be produced by the computational neuroscience discipline.

The ANNs being applied to signal processing by the author can be described as simplifying models, where underlying principles are taken from the study of real biological neural networks. This approach is aptly described and contrasted with the in-detail modeling of the actual function of biological neural nets in a recent article by Sejnowski, Koch, and Churchland.⁴ An important point from that article is the following: "Because even the most successful realistic brain models may fail to reveal the function of the tissue, computational neuroscience needs to develop simplifying models that capture important principles." At the same time, it is recognized that simplifying models can be guilty of unwarranted generalization (a human tendency). Each approach has positive and negative characteristics.

What are the principles underlying the work represented by this report? Clearly, the computing power of highly interconnected processing elements (PEs) is represented in the crossbar network, where each PE is connected to every other PE with constantly adapting efficacy. As the connections change, the network moves toward a stable state.

The way that the connectivities are determined can, in the abstract, be related to biological function. Neurobiologists have been studying an effect in biological neural systems called "long-term potentiation (LTP)", an increased (reduced) efficacy of a synapse, brought about by correlated (or uncorrelated) stimulation of the neuron or of neighboring synapses on a dendritic tree.^{5,6} Thus, the synaptic strength is a function of the correspondence of inputs. Likewise, in the beamformer, the connectivities are dependent upon the correspondence (correlation) of the inputs.

The neurobeamformer uses a matrix of covariances to determine the connectivities. This is done through the control circuitry of the beamformer which augments the crossbar circuit. The control circuit was developed out of the requirement for minimum mean square error (MMSE) at the beamformer output. This is part of the artifice which is used in the ANN, i.e., the storage of covariance is abstracted to a mathematical procedure of accumulated multiplications (the mathematical covariance) and, subsequently, the synaptic efficacy is represented by the computed conductivities of the connections, which are controlled according to the covariance values.

Covariance matrices have been used for similar purposes by signal-processing specialists in the past. Interestingly, even if the technique being used is verified to correctly represent what is happening in biological tissue, the final product which is used for signal processing loses nearly all of its biological form. Yet the technique retains the underlying principle of operation through the mathematical abstraction of covariance, and by the way

the covariance meets the requirement of the MMSE problem when a neurally inspired, highly interconnected network of PEs is used to solve it. Thus, the precept of the simplifying model is satisfied.

The use of the crossbar type of circuit for solving certain kinds of constrained optimization problems was explored by Hopfield and Tank.⁷ This work extends the optimization operation to processing in the real domain, operating mostly, or entirely, on the linear portion of the processing element response curve. The crossbar circuit is connected to a linear combiner, forming a network controlled, adaptive linear combiner or beamformer.

This adaptive beamforming method was developed by the author in the early part of fiscal year 1987. Its performance has been tested by simulation and the results of these tests are reported here.

In addition, the hardware design of these methods has been explored to the point where we have confidence that the beamformer can be implemented in the form of an analog circuit containing no control code. Thus we are able to realize experientially adaptive behavior out of the circuit architecture, obviating the need for software. Unfortunately, funding levels have not been sufficient to pursue hardware implementation.

Work has continued on a neural signal processor, the neuroprocessor, which builds upon the neurobeamformer, using it as a component in a larger network. Some elements of peripheral biological sensory systems are incorporated for the effective encoding of information, leading to enhanced spatial discrimination and adaptive cancellation of noise and interference.

What are the applications for a beamformer, or a neuroprocessor for that matter? The possibilities are many. Some examples are given in the Applications section. For the antisubmarine warfare (ASW) applications, the compactness, simplicity, and low life-cycle cost of these powerful circuits are strong motivations for further development.

3. CROSSBAR BEAMFORMING METHOD

3.1 BASIC COMPONENTS AND THEIR FUNCTIONS

The crossbar beamformer is composed of four major components (see figure 1):

- (1) Phase-shifting device for providing a phase-shifted (optimally quadrature) input for each of the channels
- (2) Controller which determines the input currents to a crossbar circuit and also the connectivities of the crossbar circuit
- (3) Crossbar network
- (4) Combiner

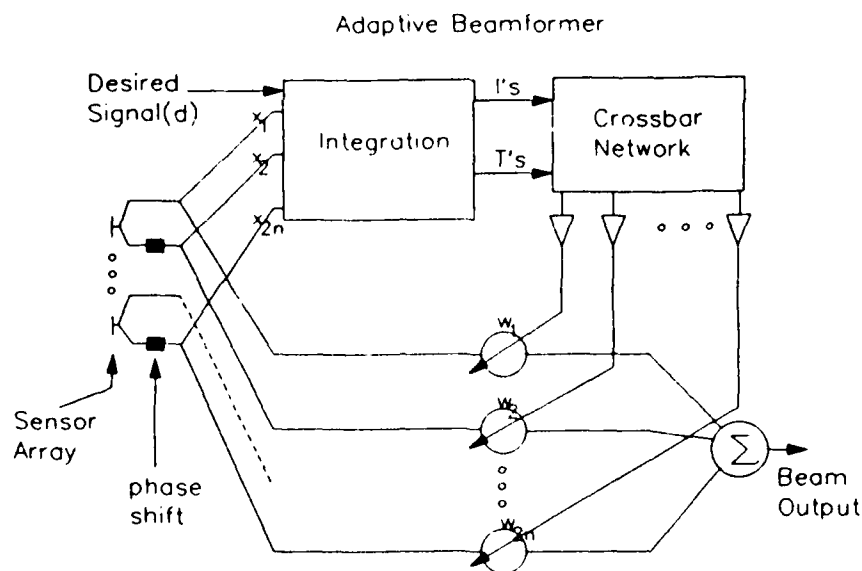


Figure 1. Adaptive beamformer.

3.2 DISCUSSION

The heart of the beamformer is the least square parameter estimator, which is a device of general applicability. This is composed of the integrator and the crossbar network, items 2 and 3 above. If an arbitrary signal time series and a set of n other time series are input simultaneously to the estimator, then n parameter value series $w_1(t) \dots w_n(t)$ are output. These parameter values are the appropriate ones to use to weight a linear sum of the n input series to form a minimum mean square estimate (MMSE) of the signal time series.

The technique of including the phase-shifted (optimally quadrature) input is a general technique for allowing any network to shift the phase of one input relative to another. In this instance, the technique is used with the parameter estimator discussed above, for the phase-shifting of inputs typical in the beamforming application.

The combiner, on the output end, does the linear sum to form the beam output. A thresholding operation could be added here, if a race for threshold with other combiners is required.⁸

3.3 NETWORK CONTROLLED COMBINER THEORY

The crossbar beamformer design was partially inspired by a paper by Hopfield and Tank,⁷ wherein they solved an optimization problem using an analog crossbar network. The key additional ideas were to use the crossbar network outputs as weights in a linear combiner and to establish a direct relationship between the beamforming error and the so-called energy function of the circuit. This being done, the circuit will endeavor to minimize its energy function, as it has been shown to do, and in the process also minimize the average squared error at the output. In this way, the optimum solution to the beamforming problem is found as the circuit converges to an equilibrium.

Figure 1 is a diagram of the total circuit. It is constructed out of a combination of five components: (1) a sensor array, (2) a device which forms a phase shifted (optimally quadrature) output from the sensor array, (3) a module which does the computation of the input currents and connection strengths, (4) the crossbar network, and (5) the linear combiner.

To better understand the meaning of beamforming error, recall that in the Widrow adaptive combiner the output(y) of the circuit (the beam output) is compared against a desired signal (d). Let the set of connection strengths $w = (w_1, w_2, \dots, w_{2n})$ be represented in matrix form by the symbol W, and the set of inputs $x = (x_1, x_2, \dots, x_{2n})$ by the matrix X. The error (ϵ) is the difference

$$\epsilon_k = d_k - y_k = d_k - W^T X_k \quad (1)$$

where the subscript, k, denotes the kth time sample of the input series. In the continuous case, it would represent the kth time. Also, the sums that are used in this discussion will be replaced by integrals in the continuous (analog) case.

The squared error is

$$\epsilon_k^2 = d_k^2 - 2d_k W^T X_k + W^T X_k X_k^T W \quad (2)$$

We wish to minimize the expectation value of the squared error, $E(\epsilon^2)$.

$$\xi = E[\epsilon_k^2] = E[d_k^2] + W^T R W - 2W^T P \quad (3)$$

where

$$\begin{aligned} R &= E[X_k X_k^T] \\ P &= E[d_k X_k] \end{aligned} \quad (4)$$

Now consider the crossbar circuit in figure 2. The energy function for the circuit is

$$\psi = -\frac{1}{2} \sum_{i \neq j} \sum T_{ij} v_i v_j - \sum v_i I_i \quad (5)$$

To have the output of the crossbar circuit determine the weights(w) of the linear combiner (as shown in figure 1), let $w_i = v_i$, $i = 1, 2n$. The input currents, I, and connection strengths, T, for the circuit shown in figure 2 are chosen so that the circuit outputs, v, are consistent with the equations above. Equating ψ and the error, and requiring minimization of the same, results in the following expressions for the Is and Ts:

$$\begin{aligned} T_{ij} &= -E[x_i x_j], \quad i \neq j, \quad T_{ii} = 0 \\ I_i &= E[d x_i] - \frac{1}{2} w_i E[x_i^2] \end{aligned} \quad (6)$$

These values continually change as the circuit adapts to its input. They will be relatively slowly changing, however, compared to the circuit time constants since they are the integrated expectation values. Thus we expect that the circuit energy function will track minima values closely when the desired signal (d) is present in the input. The following material in this section gives the detailed derivation of equation (6).

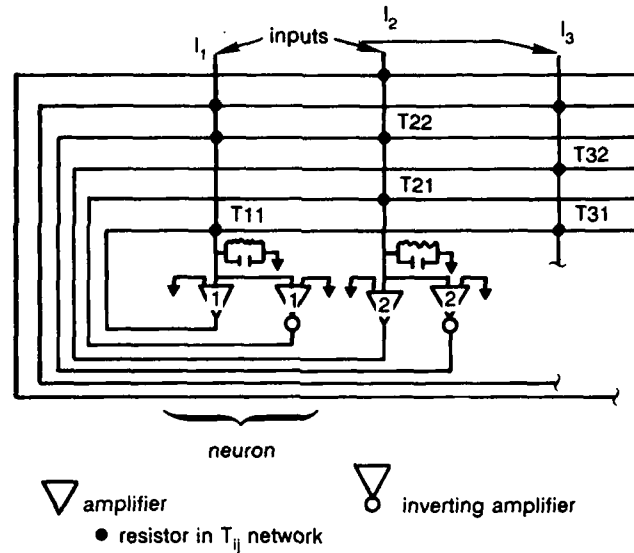


Figure 2. Hopfield crossbar circuit.

Theoretically, the crossbar beamforming device seeks the optimum least square weight matrix, W^* , in the form of voltages across the outputs of the crossbar circuit. A mathematical expression for this matrix is found analytically by taking the derivatives of the squared error, equation (3), with respect to the weights and setting them to zero. Taking the derivatives, get

$$\frac{\partial \xi}{\partial W} = \left[\frac{\partial \xi}{\partial w_0} \quad \frac{\partial \xi}{\partial w_1} \quad \dots \quad \frac{\partial \xi}{\partial w_L} \right]^T = 2RW - 2P. \quad (7)$$

Setting the derivative equal to zero, get

$$\text{optimum } W = W^* = R^{-1}P. \quad (8)$$

To complete the process, a gradient descent method is used to solve equation (8).

The circuit in figure 2 is constructed so that the energy function for the circuit (equation (5)) is a Lyapunov function. That is, as the circuit equilibrates, a minimum in the energy ([EQN "psi"]) is achieved. To assure stable behavior, the connections are kept symmetric, i.e., $T_{ij} = T_{ji}$, and the direct feedback connections are eliminated ($T_{ii} = 0$) although it is not clear that this would be necessary in all cases.

To simplify, define the following quantities:

$$\left(\begin{array}{l} \text{doubled} \\ \text{energy} \end{array} \right) 2\psi(\text{net}) = - \sum_{i,j} T_{ij} v_i v_j - 2 \sum_i v_i I_i \quad (9)$$

$$\left(\begin{array}{l} \text{modified} \\ \text{error} \end{array} \right) \psi - E[d^2] = W^T R W - 2W^T P. \quad (10)$$

Since the expected value of the desired signal remains fixed, minimization of the modified error also leads to minimization of the squared error (ψ). Next, equate the modified error and the circuit energy:

$$- \sum_{i,j} T_{ij} w_i w_j - 2 \sum w_i I_i = W^T R W - 2W^T P, \quad (11)$$

and expand the right-hand side:

$$W^T R W = \sum_{i,j} E[x_i x_j] w_i w_j + \sum_i w_i^2 E[x_i^2], \quad (12)$$

$$-2W^T P = -2 \sum_i w_i E[dx_i]. \quad (13)$$

The stated results for T_{ij} and I_i , equation (6), are arrived at by equating terms. With these values, the circuit will seek a minimum value for the circuit energy and consequently minimize the squared error. Although the values for the T s and I s are constantly changing, they are averages and consequently change slowly with respect to the time constant of the circuit.

4. ASSOCIATED NEUROMORPHOLOGY

4.1 GENERAL ORGANIZATIONAL TRENDS IN BIOLOGICAL SENSORY SYSTEMS

In general, a lot of processing is happening at the very peripheries of sensory systems, i.e., in the immediate vicinity of, or within, the sensor and supporting structure, where the data are encoded or translated, into the language of the neuropile. In the process, relevant information is preserved, and what is relevant is determined by feedback from processing. The adaptive beamforming operation is quite analogous in this respect.

During neural encoding, the stimulus is transformed in various ways to reveal and separate patterns and features. Studies of vision in monkeys indicate the existence of segregated pathways, differing in their selectivity for color, stereopsis, movement, and orientation,⁹ beginning at the earliest peripheral stages in the visual system and persisting into the higher levels, where memory, modeling (generalization), and control occur.

Studies of the auditory system in cats reveal encoding which forms in at least three-dimensional representation of the stimuli. These are suggested by Geisler¹⁰ to be average discharge rate, temporal discharge pattern, and tonotopic place. Greenberg¹¹ suggests rate/place, synchrony/place, synchrony/quasi-place, and synchrony/place-independent as bases for neural encoding.

4.2 AUDITORY CROSS-CORRELATION MODELS

Auditory systems in animals extract information from a variety of sounds, from machinery noise, to music and speech. Several models of binaural auditory information processing have included computation of cross-correlation and covariance.^{12,13,14,15,16} Deng, et. Al.,¹⁷ include what they call cross-channel correlation in their model of monaural speech processing.

In applying these models of auditory processing of speech-induced signals to sonar signals, one presumes that the neural encoding schemes represented in the models are not specialized to speech exclusively. This is probably a safe assumption because of requirements for efficient use of neural matter in these systems.

Many of the effects which the sonar signal processor must account for are also considerations in auditory processing in humans, cats, dolphins, and bats. For instance, the effects of multipath on hearing have been studied,¹⁸ and so has the reduction of recognition performance in the presence of masking noise.

5. SUGGESTED EXTENSIONS

5.1 A DEMONSTRATOR

Some preparations have been done to build a demonstrator using the combination of a microphone array and the neurobeamformer simulator as a starting point. A microphone array with nine separate input channels has been acquired and the ANZAs (Zenith 386 machines containing the Hecht-Nielsen 68020-based coprocessor boards) have been outfitted with analog-to-digital conversion devices. It remains to be seen if the ANZAs will have sufficient power to make the demonstrations realtime enough for presentation at a meeting. If not, a faster processor will be found or the demonstrations can be videotaped.

It has been proposed that this demonstrator could also serve as a testbed, where pieces of the simulator would be replaced with hardware in a step-by-step manner in order to keep problems isolated. The first configuration would have a microphone array interfaced via the preamplifiers to the neurobeamformer simulation. During this phase, the correct operation of the array and successful processing of its signals by the digital implementation could be verified.

Next, a hardware version of the integration for establishing the covariance matrix could be constructed and introduced between the array and the computer. A portion of the digital code would be displaced and the demonstrator would be speeded up. With the operation checked out just prior to the change, any problems would be associated with the new piece or the way that it was interfacing. Also, previously recorded intermediate values could be compared with the outputs of the newly introduced hardware.

This process can be continued by introducing a crossbar very large scale integration (VLSI) chip, and displacing another portion of the digital implementation. At this point the digital computer would be used as merely a data acquisition device. Finally, the microphone array itself could be replaced with hydrophones for tests at-sea.

5.2 NEUROPROCESSOR

The "neuroprocessor" is a proposed extended network which builds upon the adaptive beamformers. One simple extension is to impose a layer of neurons between the sensor quadrature inputs and the parameter estimator and between the inputs and the combiner. Thus, the inputs to the estimation process are a coarse sampling of the phase pattern space. The coarseness is determined by the beamwidth of the individual input neurons.

There is an information-coding scheme known as the "coarse-coding scheme", and it is found, for instance, in the auditory system. Figure 3 shows the overlapping frequency response curves for individual neurons in the peripheral auditory system as an example. These overlapping filters can be thought of, by analogy, as beams in frequency space.

Figure 4 shows analogous, overlapping cookie-cutter beam patterns. By applying Boolean logic to these, regions are defined by a pattern of combined responses. The region $A \cap B \cap C$ is illustrated.

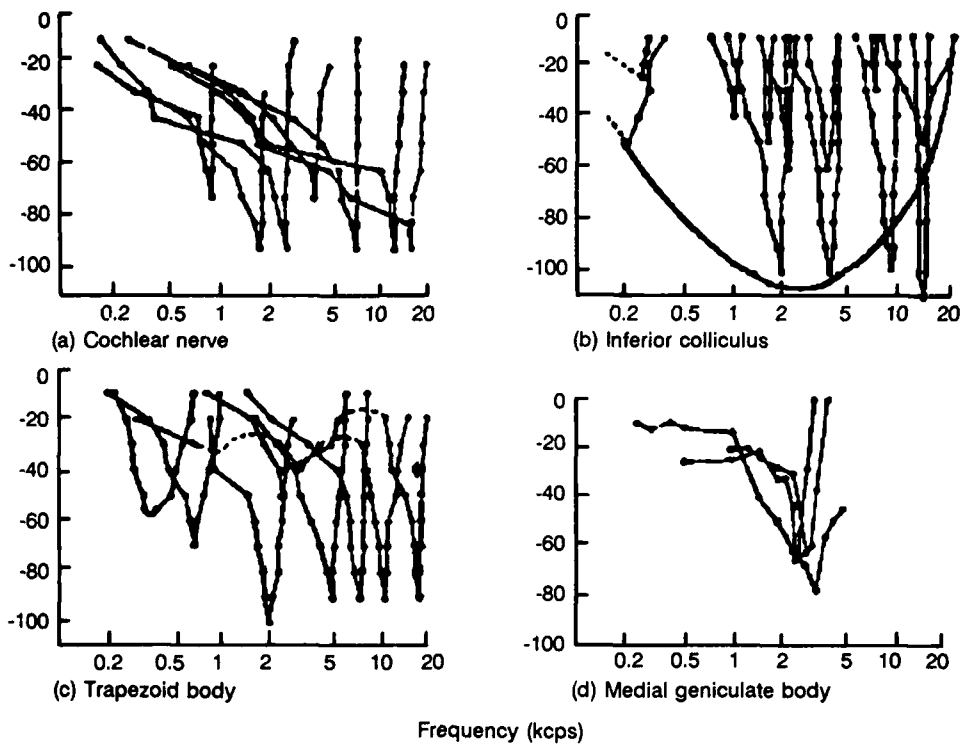


Figure 3. Response areas of single neurons of the peripheral auditory system of the cat.

Coarse Coding for Pattern Generation

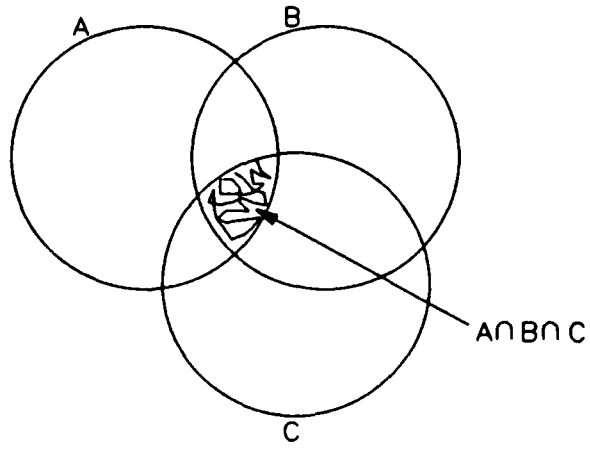


Figure 4. Venn diagram of beam patterns.

In the real case, the beams will have sidelobes, which makes the logic more complex. But, we will also have an adaptive combiner to determine the correct mix, i.e., figure out the coarse coding. The weights, which compose the mix, form patterns. A backpropagation network will be trained to associate the patterns with a direction estimate. Thus, a coarse-coding scheme will be utilized to achieve a high degree of resolution, although the individual beams, due to their width, do not resolve very well.

The subject weights which form the pattern for direction estimation are also used for combining the beams into a composite beam for enhancing the desired signal and rejecting interference.

5.3 TARGET LOCATOR

The target locator overview plan is shown in figure 5. It will include the functions performed by the neuroprocessor discussed above and, in addition, do target recognition. That is, there are some echo-signature techniques and signal-decomposition techniques that can be utilized to determine the identity of the signal/echo source.

Figure 6 shows a more detailed diagram of how the networks may be permuted and combined to perform the recognition function. This includes a form of lateral inhibition and a signal decomposition according to a set of basis functions. The lateral inhibition allows for a partitioning of the input space, where neighboring beams claim inputs and exclude other beams from training on them.

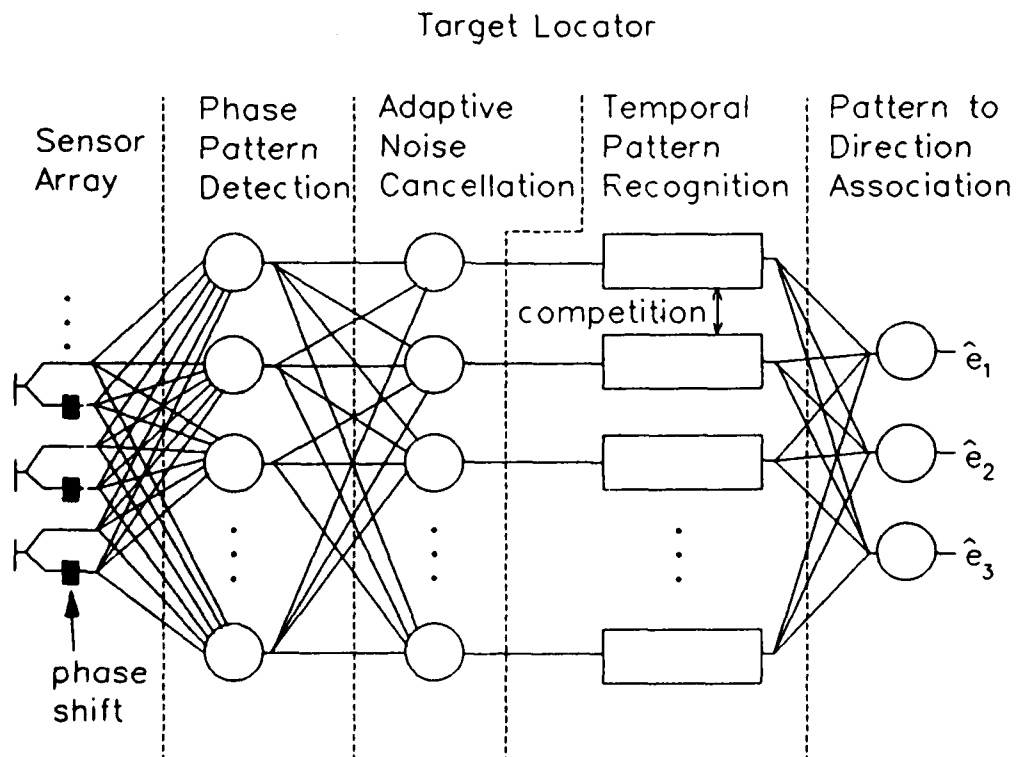


Figure 5. Overview plan for the target locator.

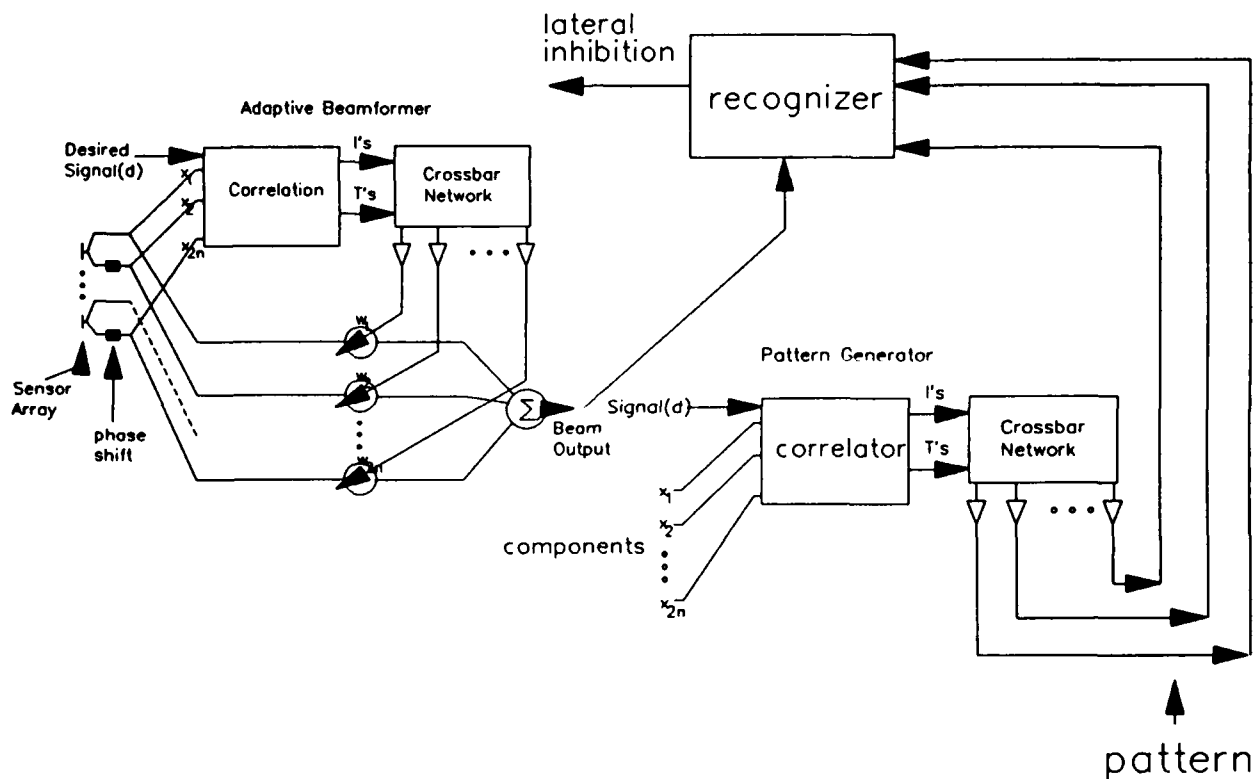


Figure 6. Lateral interaction technique for target locator.

6. DISCUSSION OF TEST RESULTS

6.1 THE SIMULATOR

To do the tests, simulation code was written on the ANZA. Data preparation, such as merging reverberation and SEG outputs, was accomplished on a VAX/780 and the files were subsequently downloaded to the ANZA (figure 7).

6.2 THE DATA

The data used for these tests are taken from nine summed rows of an array, which was immersed 30 meters deep in Dabob Bay and traveling at 15 knots. The bay depth was approximately 200 meters.

Ultimately, it was realized that the data files received from Marine Physical Laboratory (MPL) have been altered by a rotatory tion of the complex samples. The data were de-rotated to eliminate the change in the data spectral characteristics.

Additional (surveillance) data are available and have been successfully read and converted for testing the neural networks. Analysis using the Dabob data has suited required testing up to this point. Test results on surveillance data will appear in a later report.

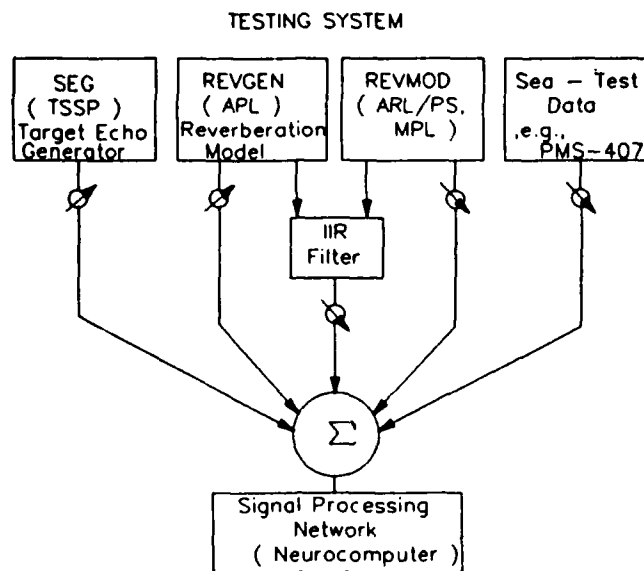


Figure 7. The testing system.

6.3 THE RESULTS

Tests indicate that the adaptive beamformer method, based on neural network technology, performs the desired function of directing a beam so as to enhance a target signal and cancel noise and interference. The interference-cancelling performance of the method has not yet been quantitatively compared with other methods, but it is clear from the tests reported here that the performance is good.

It has been noted, from comparison of the test output values and a matched-correlator output, that the plotted crossbar circuit energy minima follow the shape of an inverted matched-filter output. This makes sense if we look at how the connectivities and the currents are computed from the signal, and their role in the energy equation. The energy is

$$\Psi = -\frac{1}{2} \sum_{i,j} \sum_{i',j'} T_{ij} v_i v_j - \sum_i v_i I_i \quad (14)$$

where the connectivities are related to the autocorrelation matrix

$$T_{ij} = -E[x_i x_j] \quad (15)$$

and the input currents are related to the cross-correlations of the channels with the desired signal (d) and the weighted autocorrelations

$$I_i = E[dx_i] - \frac{1}{2} w_i E[x_i^2]. \quad (16)$$

If we combine the equations to get the expanded energy equation, we get

$$\Psi = -\frac{1}{2} \sum_{i,j} \sum_{i',j'} (-E[x_i x_j]) v_i v_j - \sum_i v_i E[dx_i] + \frac{1}{2} \sum_i v_i v_i E[x_i^2]. \quad (17)$$

It appears that during the target return the second term above can dominate. It is the only term which is not multiplied by the square of the outputs, v_j , which are often small.

The neurobeamformer has certain advantages of implementation and adaptability over other methods. It is, in concept at least, implementable in analog circuitry with no control code required. This allows a compact, simple, low-cost processor component to be produced. Also, the method is not sensitive to array grooming as are some of the other available methods.

To summarize the results of the tests, for synthesized target echoes, the beamformer points a beam, of width and character determined by the array spacing and aperture, directly at the target and it leaves it there for a period of time approximately equal to twice the duration of the target echo. It does so at SIR as low as -15 decibels. Below this value, there are problems discriminating the target from the interference in the case where the target-echo spectrum is overlapped by the interference spectrum. This overlap happens, for example, when the target is stationary. In the case where the target is in motion with respect to the medium of approximately 15 knots in the general direction of the receiver, the beamformer performs well down to an SIR of -30 decibels.

It is recognized that a straightforward adaptive beamformer cannot match the interference-cancellation performance of more exotic methods which include sidelobe cancellers, etc.^{1,2,3} Therefore, a neuroprocessor will be constructed which incorporates the neurobeamformer as a component that will provide for cancellation of sidelobes, enhanced source discrimination and angle estimation through interaction of beams. The plans for this extended network were influenced by studies of the literature in biological sensory processing, peripheral and central.

6.4 EXAMPLE TEST OUTPUTS

The example test runs show two major cases (1) the target echo is not overlapped with the reverberation ridge and (2) the target echo is completely within the reverberation ridge.

In the first case, the target has an up-Doppler shift representing approximately 15 knots of target speed. Figures 8a, 8b, and 8c show time-Doppler contour plots of the interference, the target echo, and target plus interference respectively. The target echo is essentially a point target return. The pulse duration is 180 milliseconds.

Figures 9a and 9b show time histories of the beamformer sensitivity versus angle and the crossbar network "energy" (defined in equation 5 and expanded in equation 16) for when the interference only is processed by the network.

Figures 10a and 10b are similar to figures 9, except that the target echo is present at -30 dB SIR. The target is a point target traveling at 15 knots toward the receiver. Notice the pronounced dip in the energy function values as compared to the figure 9b. Also notice the increased sensitivity at the target angle and reduced sensitivity at other angles.

Figures 11a, 11b, and 11c are similar to figures 8, showing time-Doppler contour plots for interference only, target echo, and target plus interference. Its Clearly, the target echo and interference overlap. The SIR is 0.0 decibel. The following figures are for this case of a stationary target with commensurately overlapped interference and target-echo spectrograms.

STANDARD ECHO GENERATOR
Time-Doppler Contours

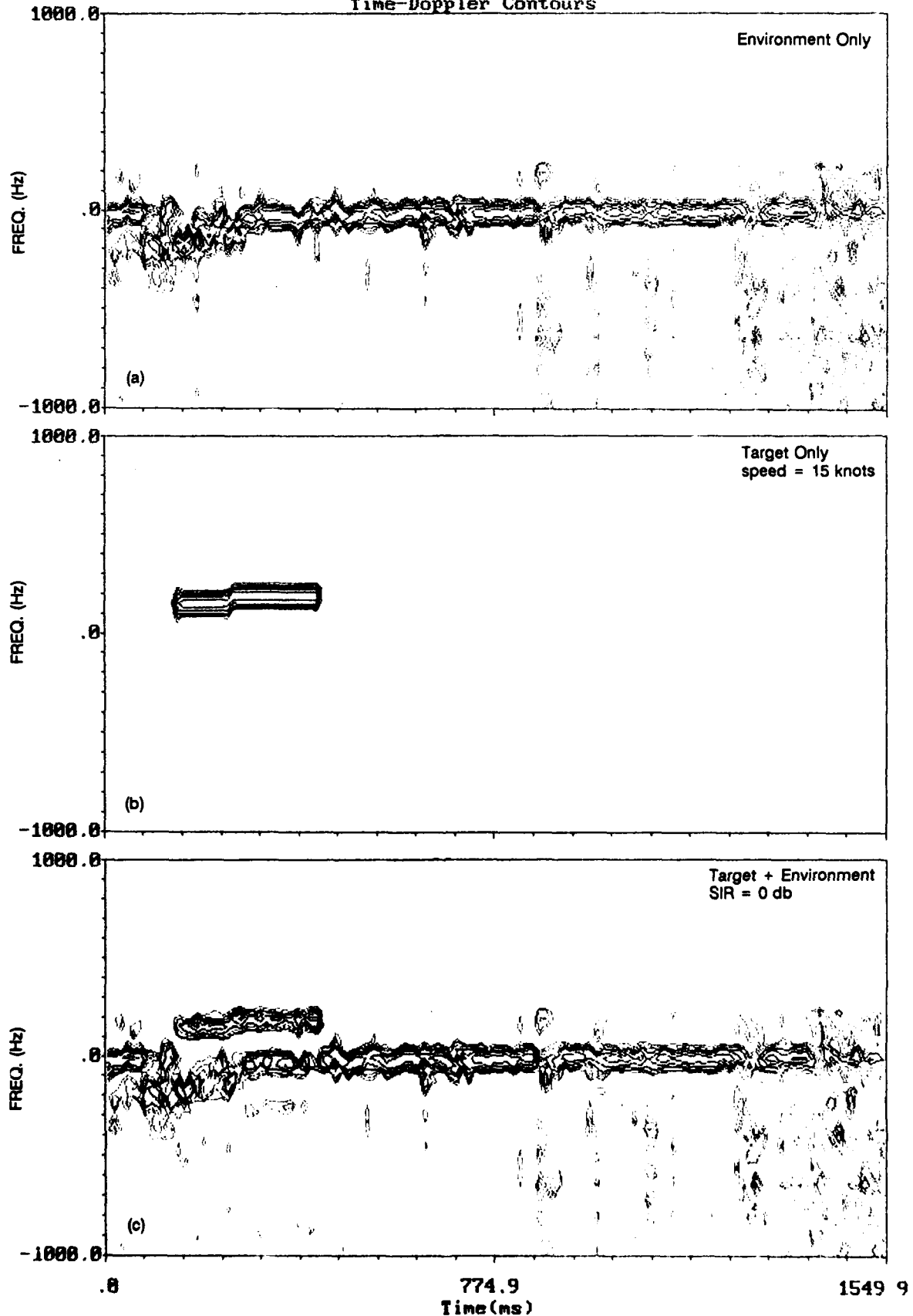


Figure 8. Spectrograms of down-translated signals: (a) Interference only, (b) target only, speed = 15 knots, (c) target & interference, SIR = 0 dB.

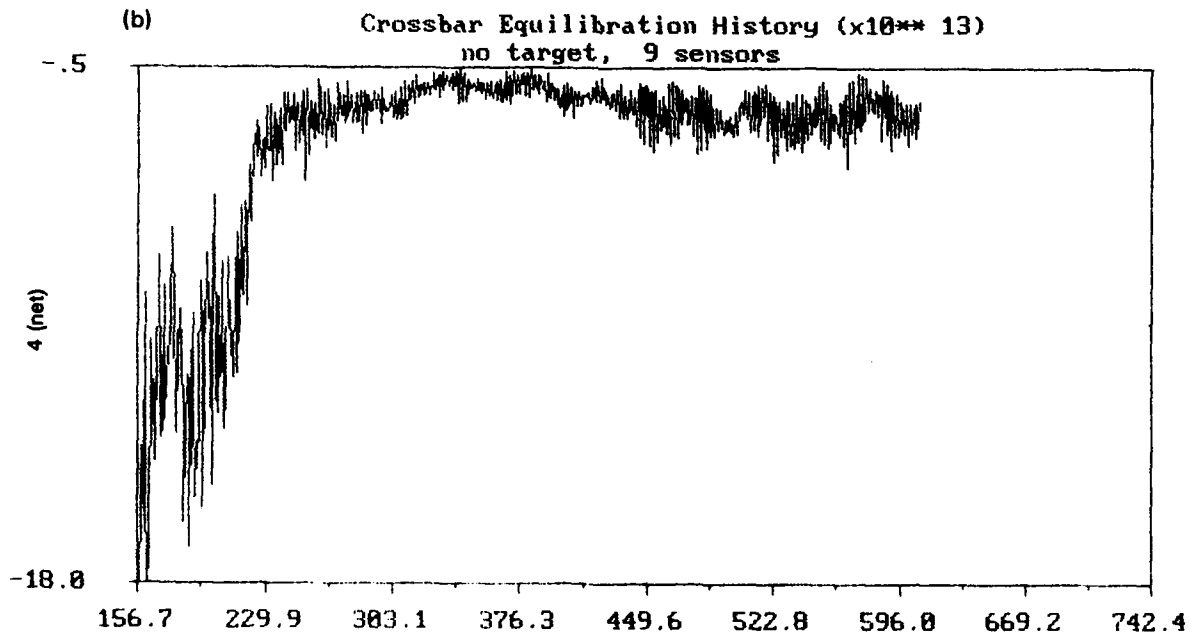
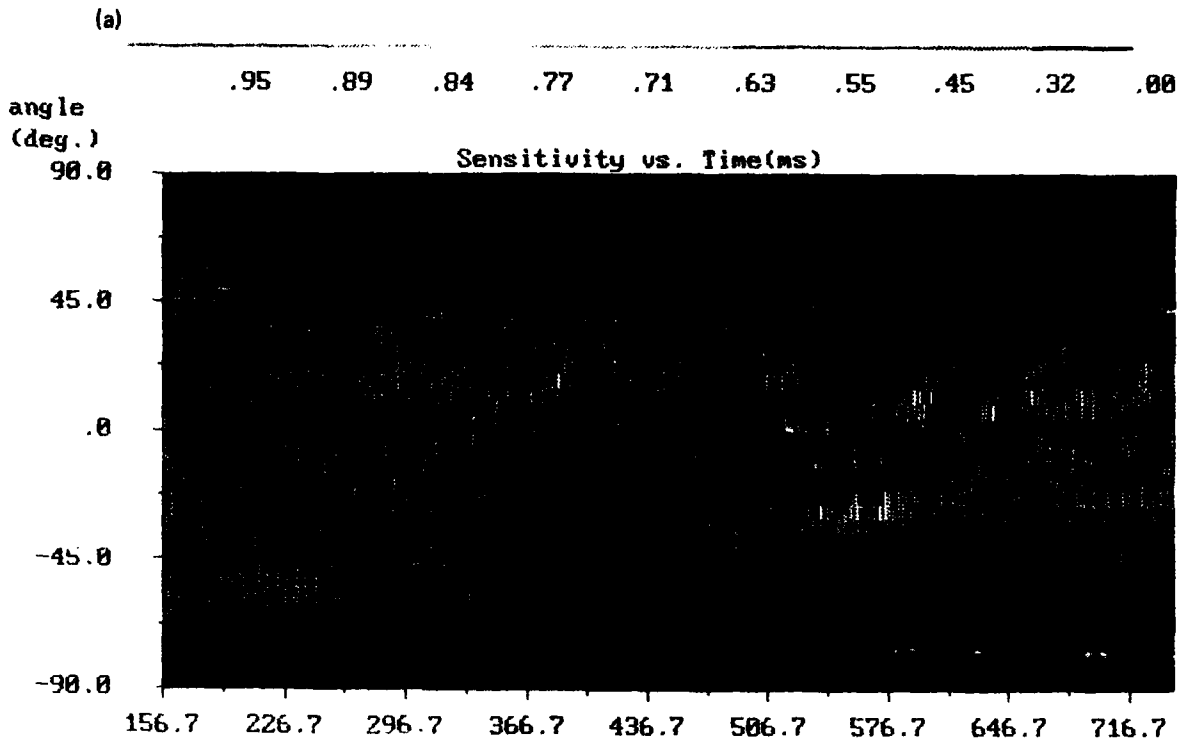


Figure 9. Sensitivity and crossbar energy histories for case of no target, interference only.

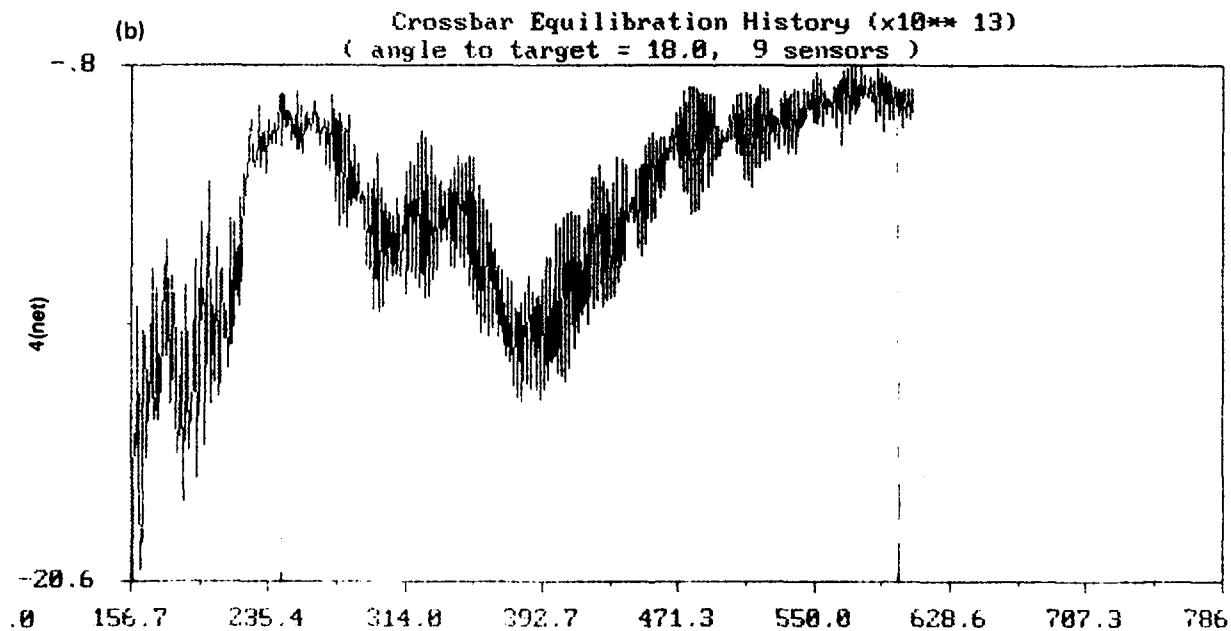
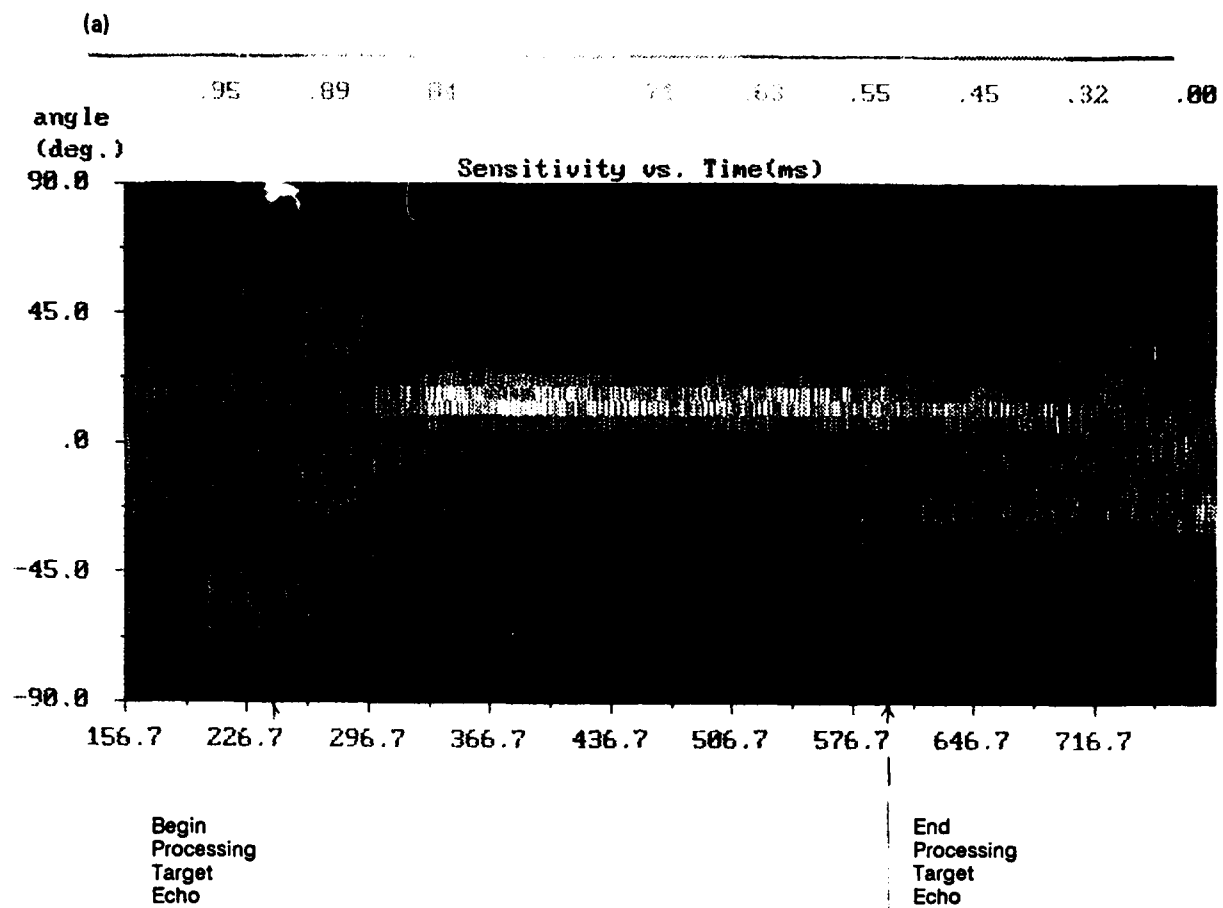


Figure 10. Sensitivity and crossbar energy histories for case of point target, SIR = -30 dB, speed = 15 knots; interference same as figure 9.

STANDARD ECHO GENERATOR

Time-Doppler Contours

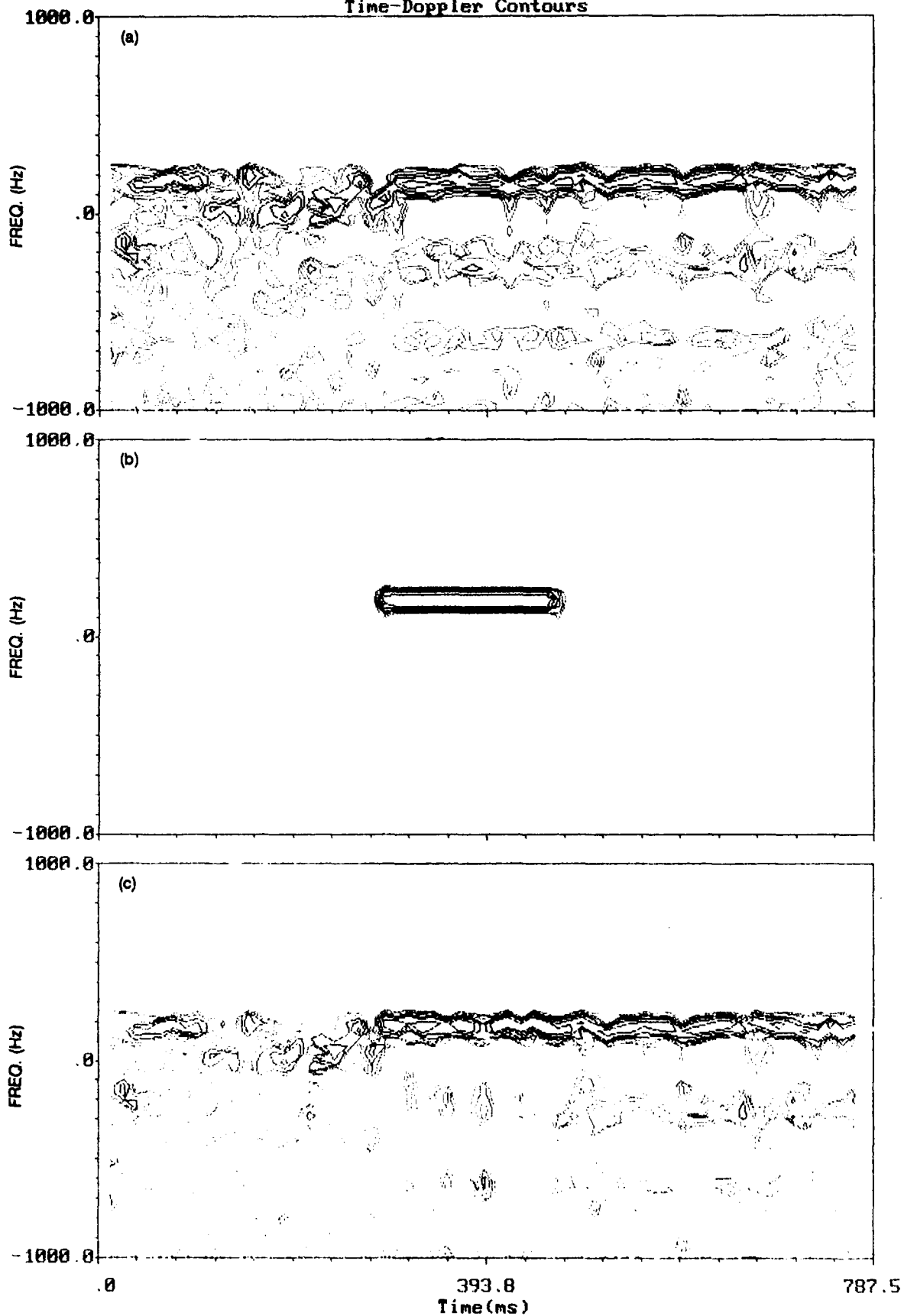


Figure 11. Spectrograms of down-translated signals:(a) interferences only, (b) target only, speed = 0 knot, (c) target & interference, SIR = 0 dB.

Figures 12a and 12b show the time history for the beamformer sensitivity versus angle, for this case of a stationary target. The beamformer is again becoming attentive to the target angle. The author has noticed that there seems to be more training on the interference in this case. There is yet no explanation to this phenomenon.

Figures 13a and 13b show the crossbar network energy. It dips to a minimum when the desired signal is present. Figure 14a shows the beam output and one of the corresponding input channel time series. Figure 14b shows the matched-filter output, produced by correlating the desired signal with the streams shown in figure 14a.

Figures 15a and 15b show snapshots of the evolving beam, plotted in a polar format. The beam is initialized to look in the forward direction (the black curve). Subsequently, as the environmental echo comes in, the beam thrashes about in the color red, which signifies a crossbar energy. When the target echo comes in, the color changes to blue, signifying a dip in the crossbar energy, and the beam is seen to be well-formed in the proper direction. Figure 16 shows some of the connection strength histories corresponding to this run. The rest of the set is contained in appendix A.

Figures 17 and 18 show the histories for input currents 1 through 18 shown in the crossbar circuit diagram, figure 2. The currents show an oscillatory nature, which can be understood by inspection of equation 16. The first term is related to the cross-correlation of the input with the desired signal. In this case, both of the series contain Doppler ripple, resulting in the oscillation. If both series had been frequency-shifted to compensate for the platform motion (which is often done in signal processing schemes), then the currents would show less oscillation.

Figures 19a and 19b show bargraphs of the ranges of the connection strength values and the current values respectively. These ranges are important when considering hardware constraints. The connection strength values are shown as conductivities (mhos), and indicate that the variable connections must operate in the range of open circuit to approximately 25 ohms resistivity.

Figure 20 is the first in the set for an SIR equal to -15.0 decibels. It shows the sensitivity history. Figures 21 through 24 show the crossbar energy, polar beam plots, beam output, and connection strengths respectively. It is evident that the target echo is indistinguishable from the interference by visual inspection alone and if one did not already know where it was. However, when watching the evolving polar plots, the author found it interesting that the beam was more well-formed, in terms of its width and sidelobe characteristic, during the target return than during the interference. The beam color only reaches yellow in this case, making it more difficult to distinguish from the previous patterns on the plot.

Comparison of figures 24 and 16 shows that the connectivity histories are very similar for the runs with SIRs of -15 decibels and 0 decibels respectively. Note the scale change.

Figure 25 is the first figure of output for the case where the target is a multiple highlight target. Figures 26 through 29 are for the same case. The main difference from the point target case, at the same SIR, is that there is a secondary broad energy minimum. This may be due to the spatially extended nature of the target. It is not known why the beam trains strongly at the beginning of the run.

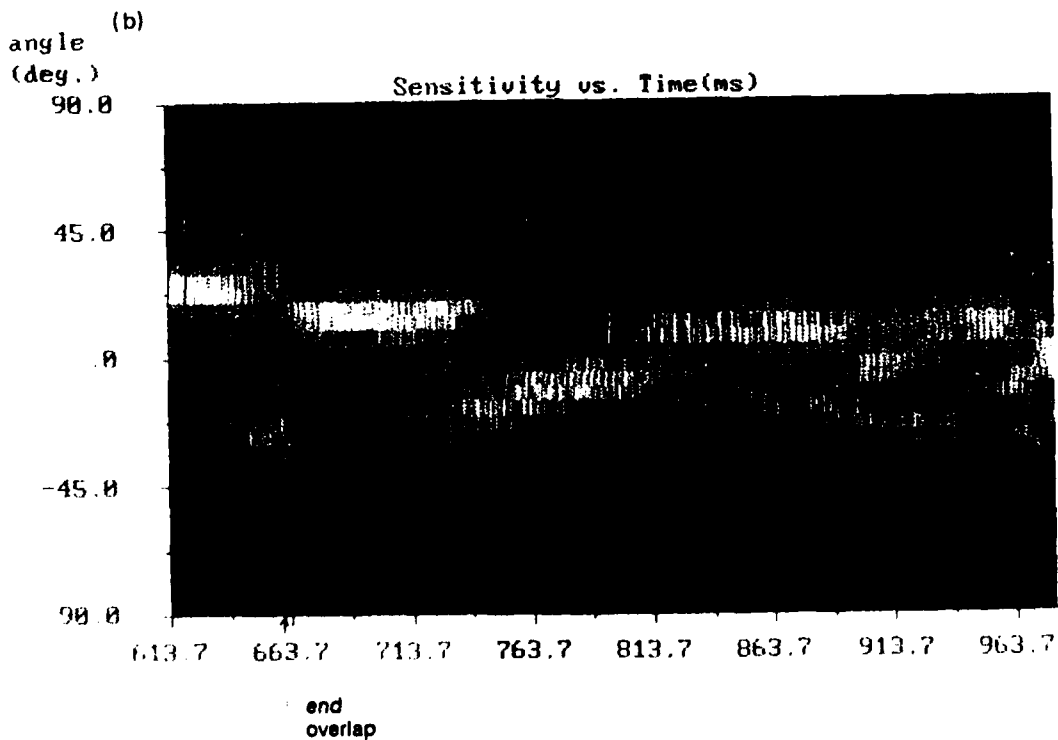
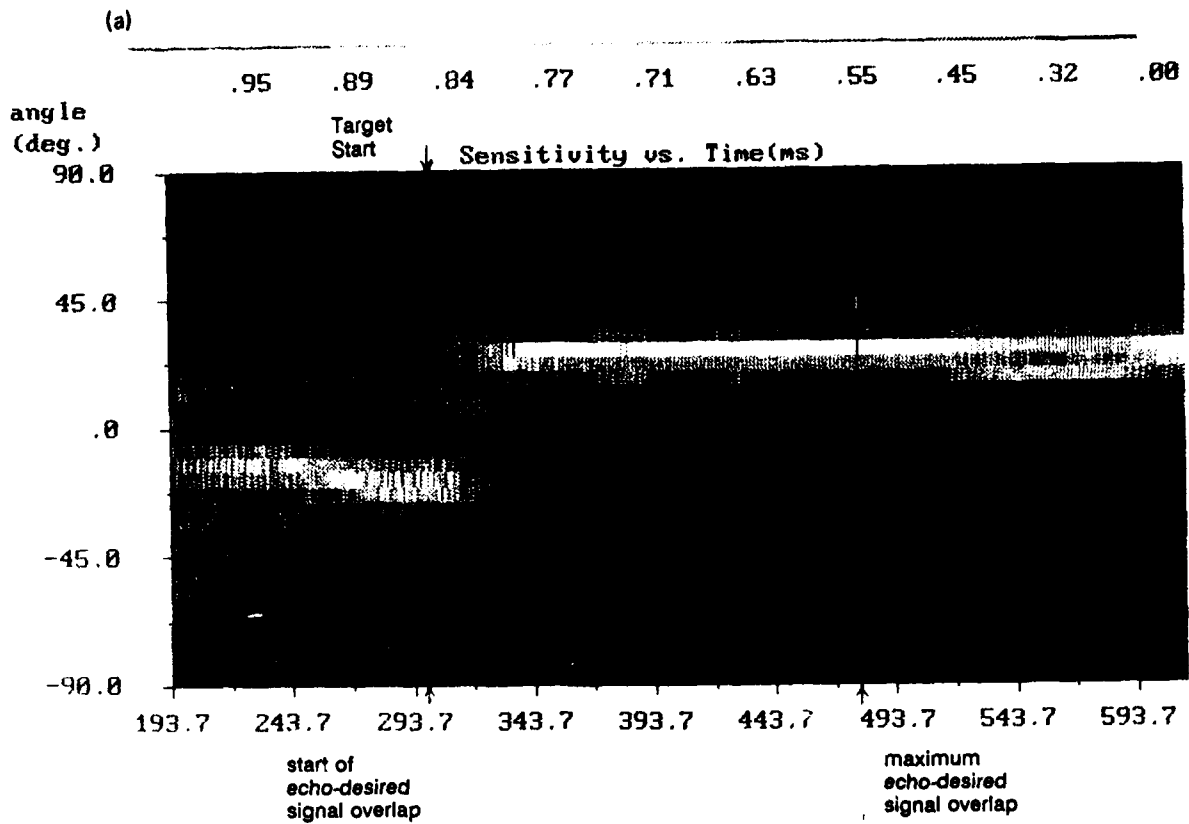


Figure 12. Sensitivity history for point target at SIR = 0 dB, speed = 0 knot.

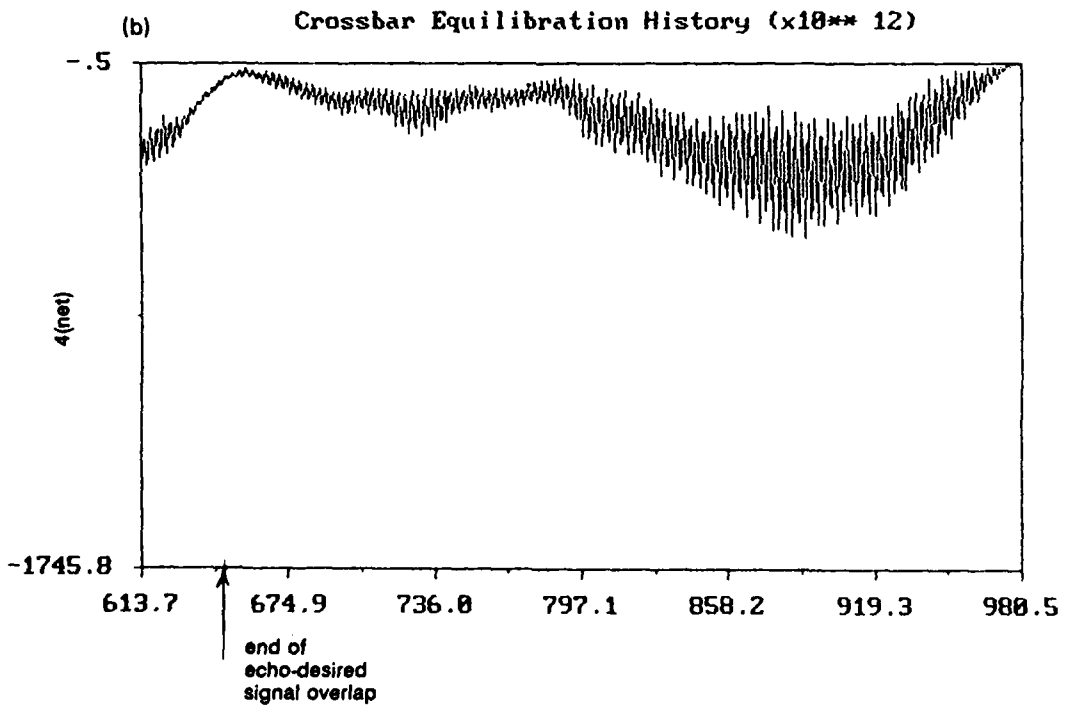
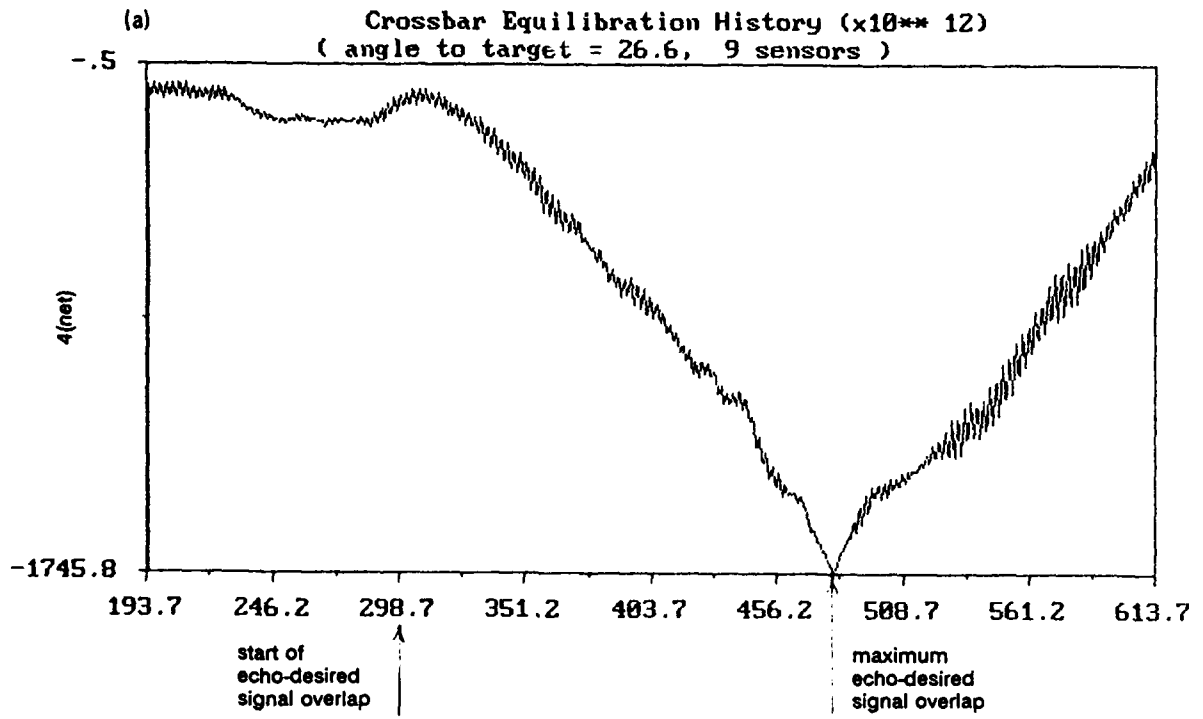


Figure 13. Crossbar network energy history for point target at SIR = 0 dB, speed = 0 knot.

(a)



(b)



Figure 15. Snapshots of evolving/adapting beam: (a) before target echo return
(b) after target echo return. Red is high energy, blue is low energy.

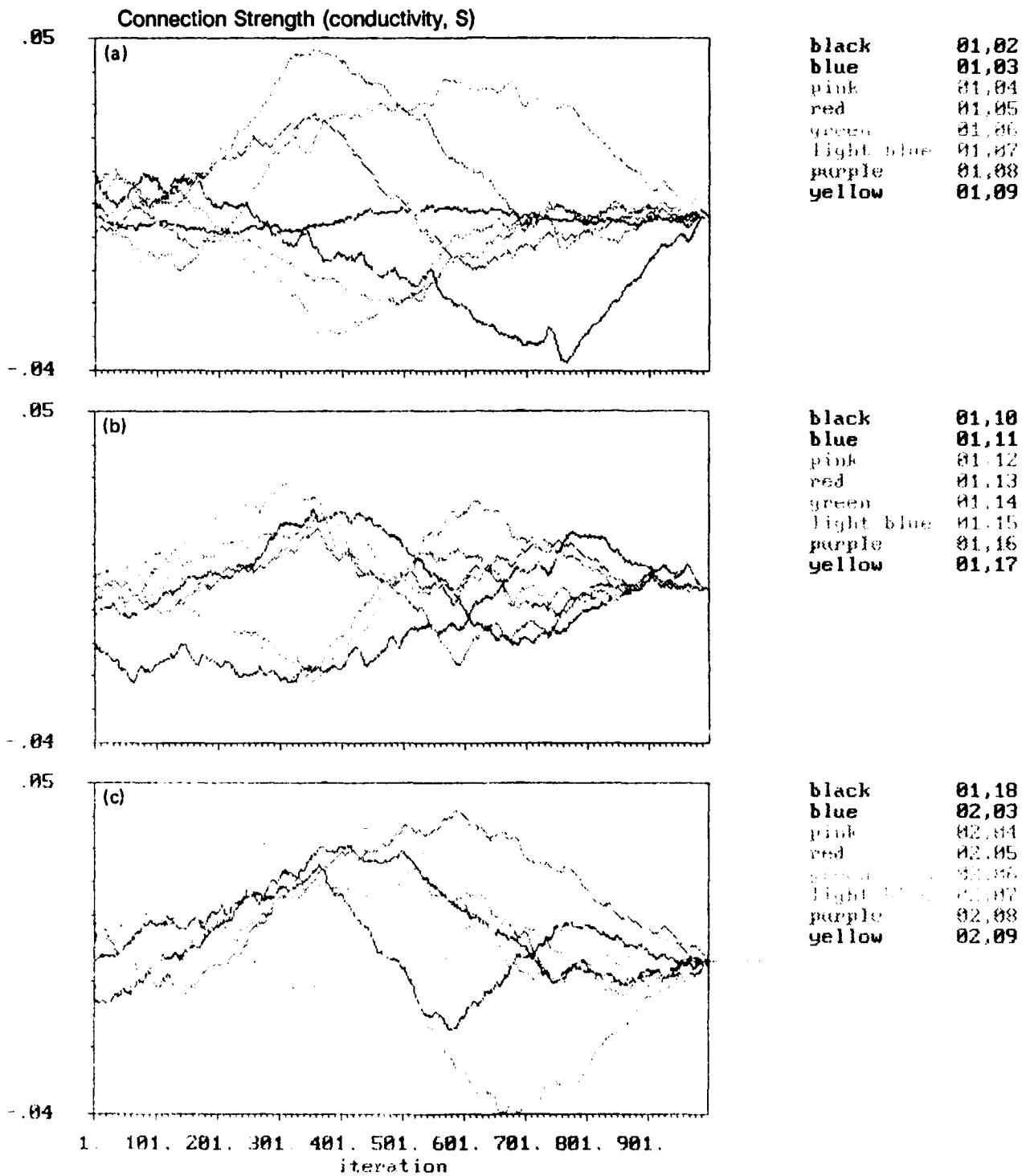


Figure 16. Connectivity histories for case of point target and SIR = 0 dB (iteration \approx 0.8 ms)

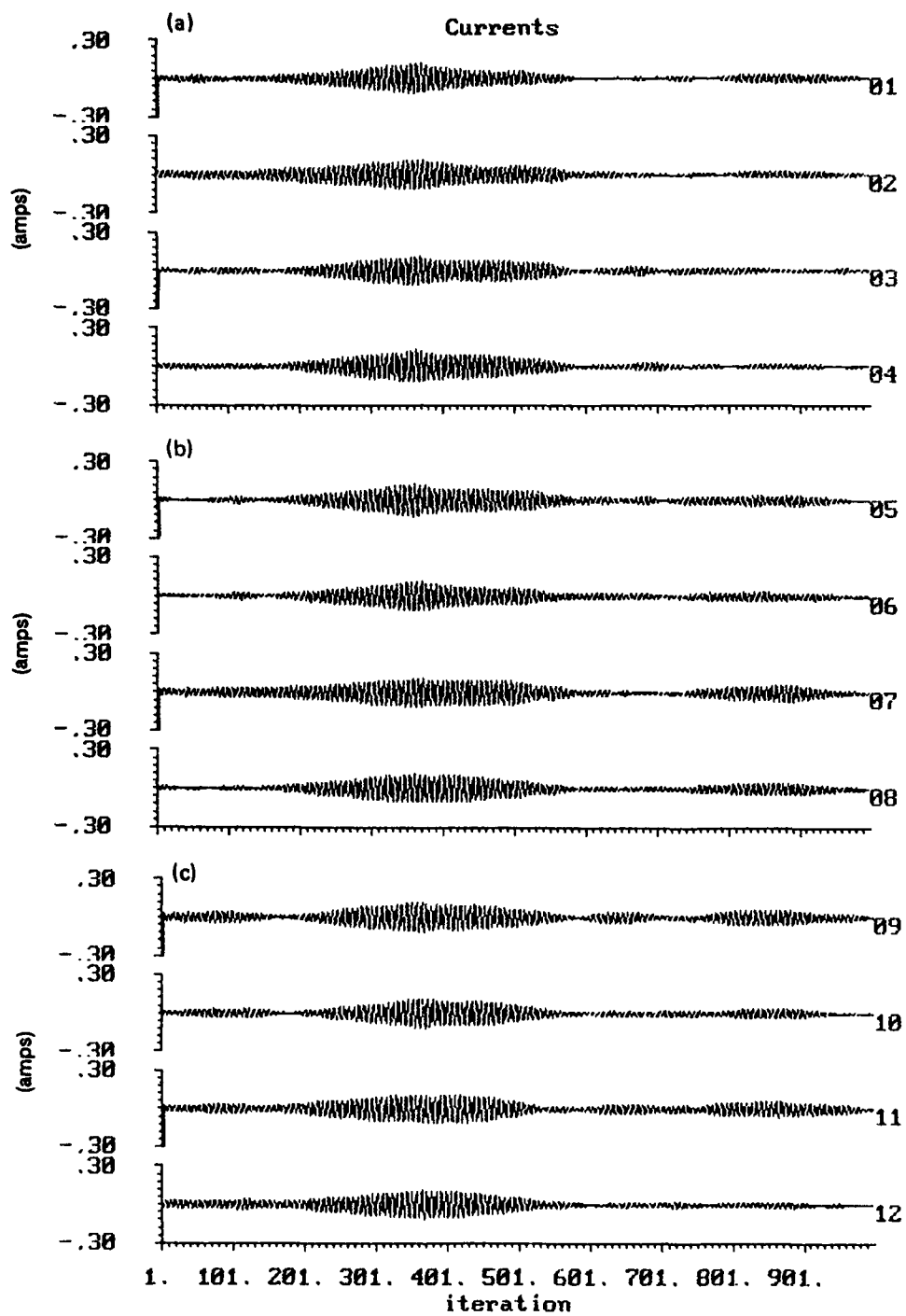


Figure 17. Input current histories for point target,
SIR = 0 dB (iteration \approx 0.8 ms)

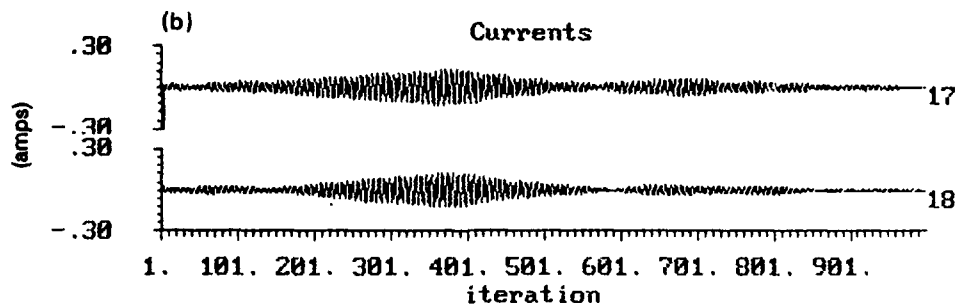
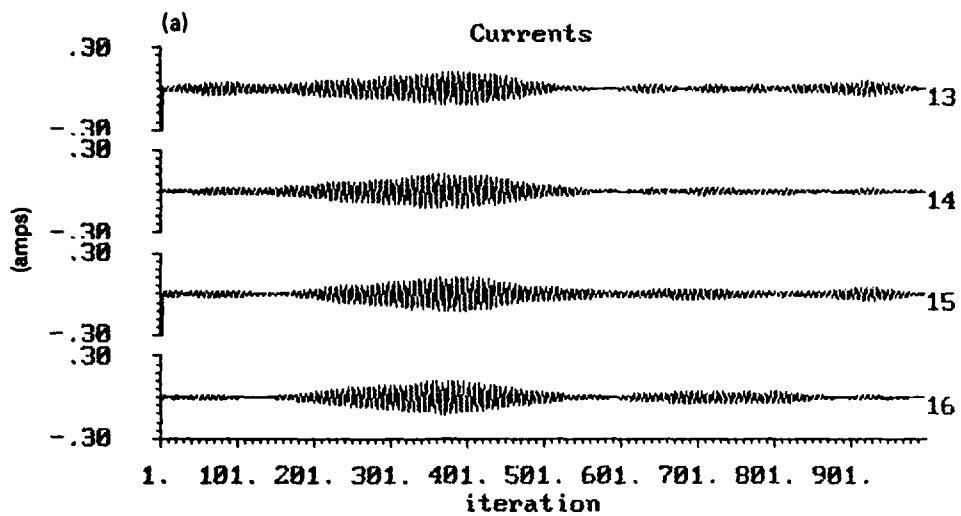


Figure 18. Input currents (continued from figure 17.
iteration \approx 0.8 ms).

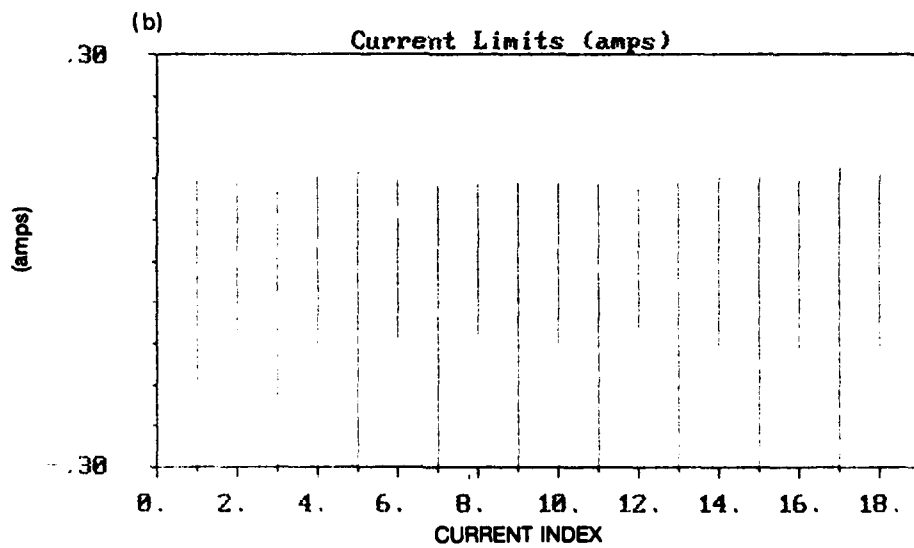
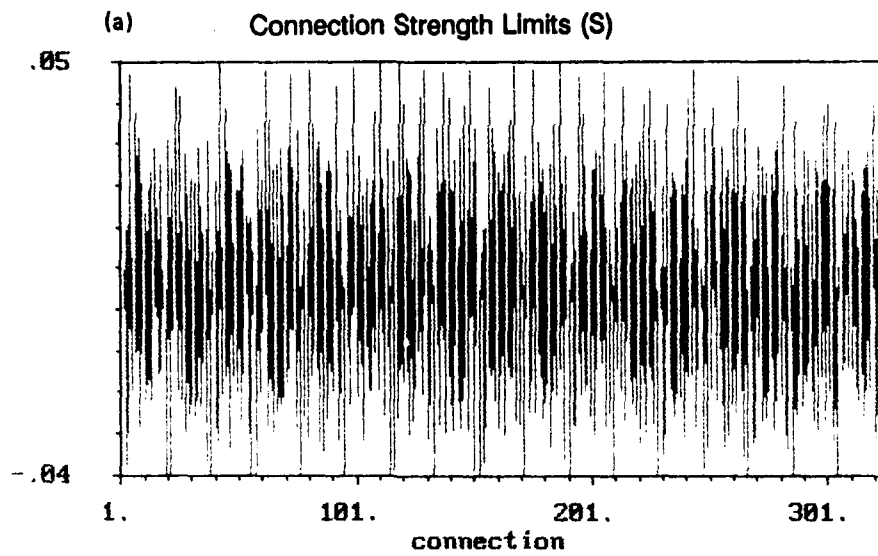


Figure 19. Connection strength and input current value ranges for case of point target and SIR = 0 dB.

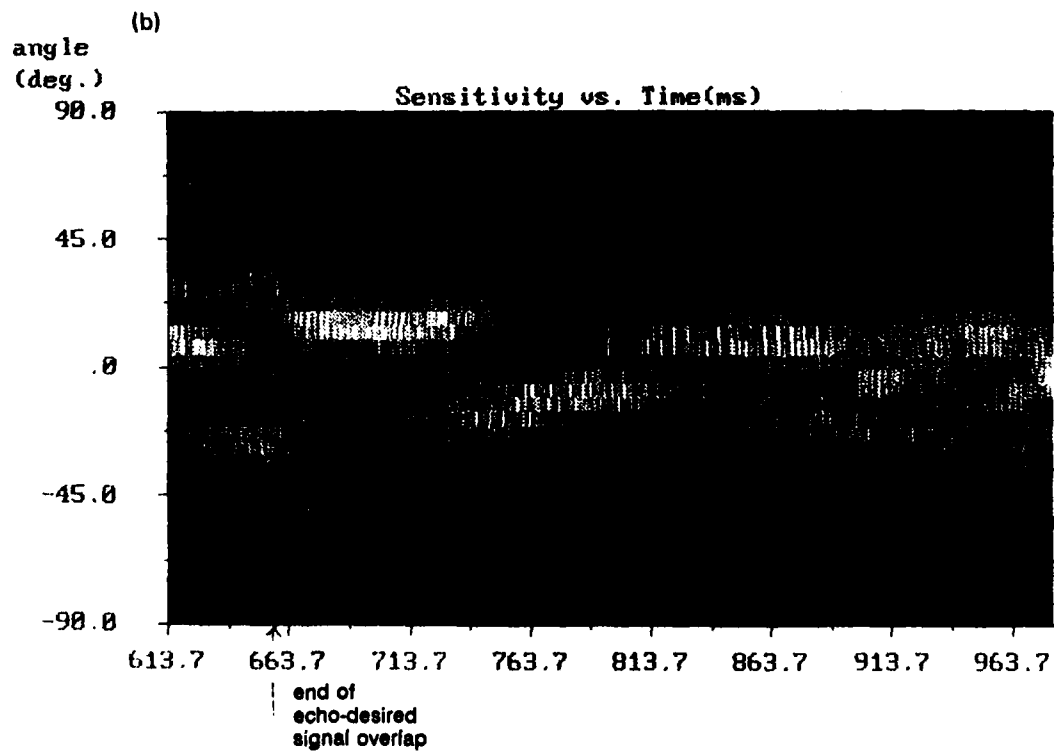
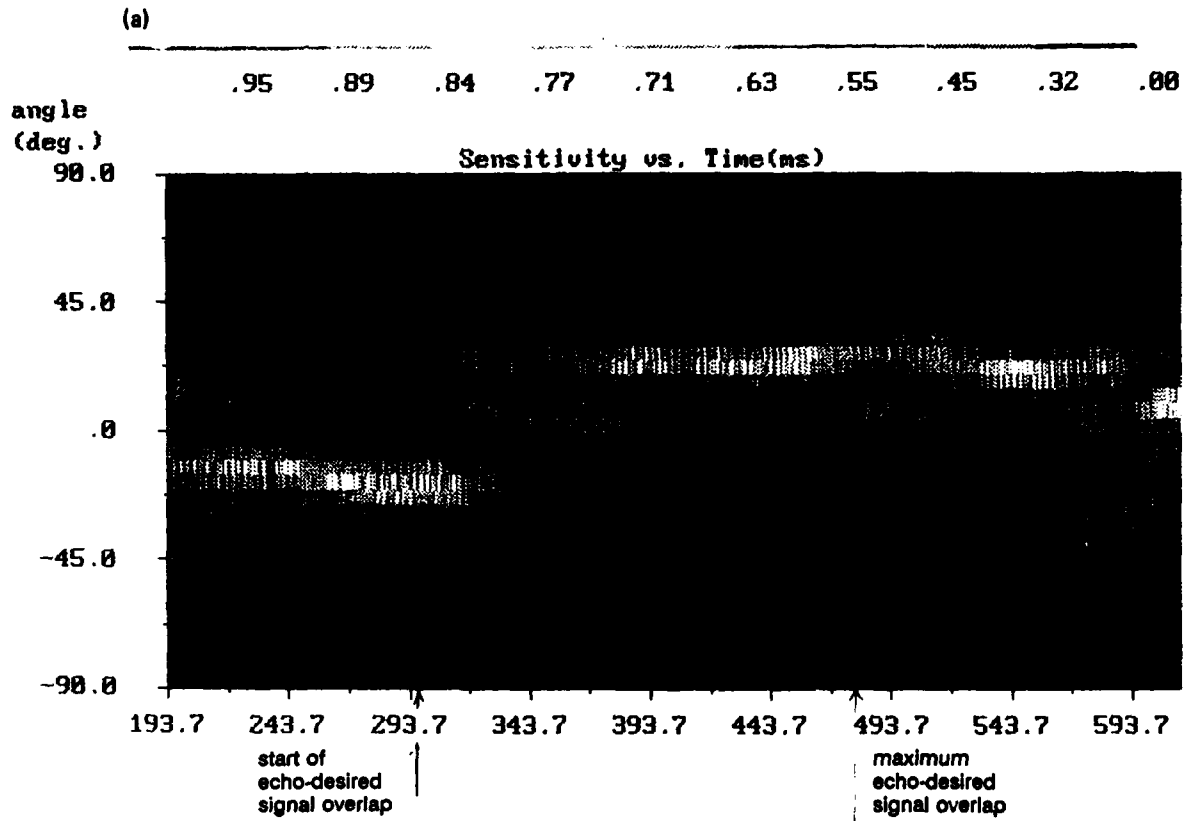


Figure 20. Sensitivity history for case: point target, SIR = -15 dB, speed = 0 knot.

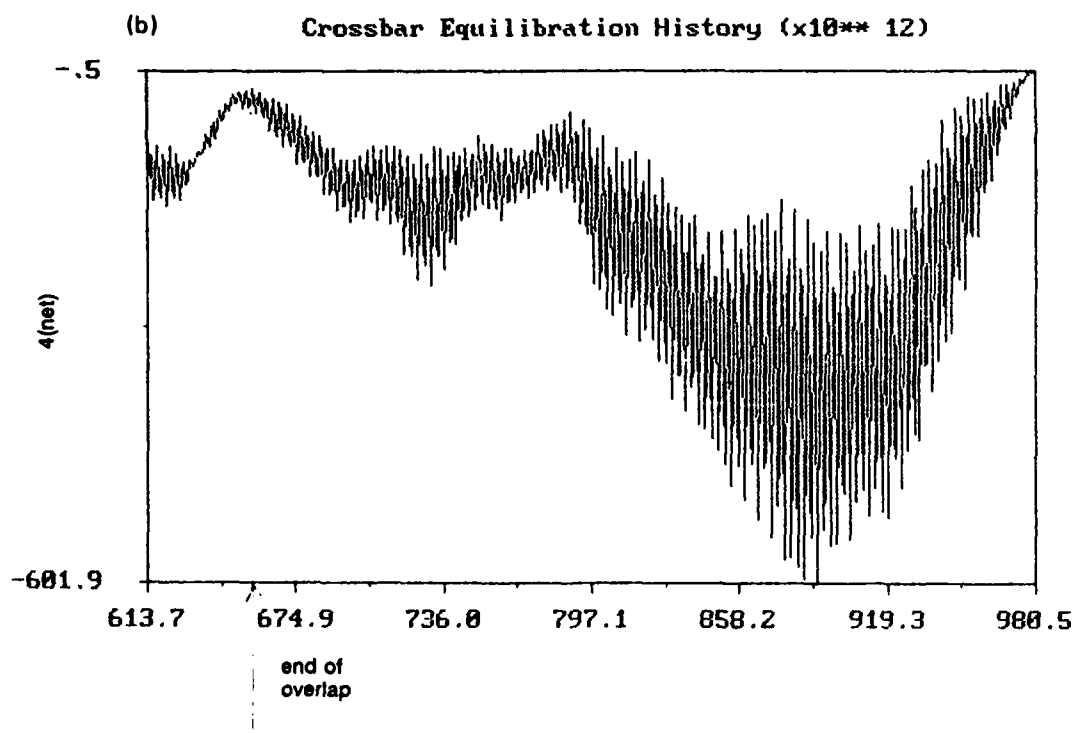
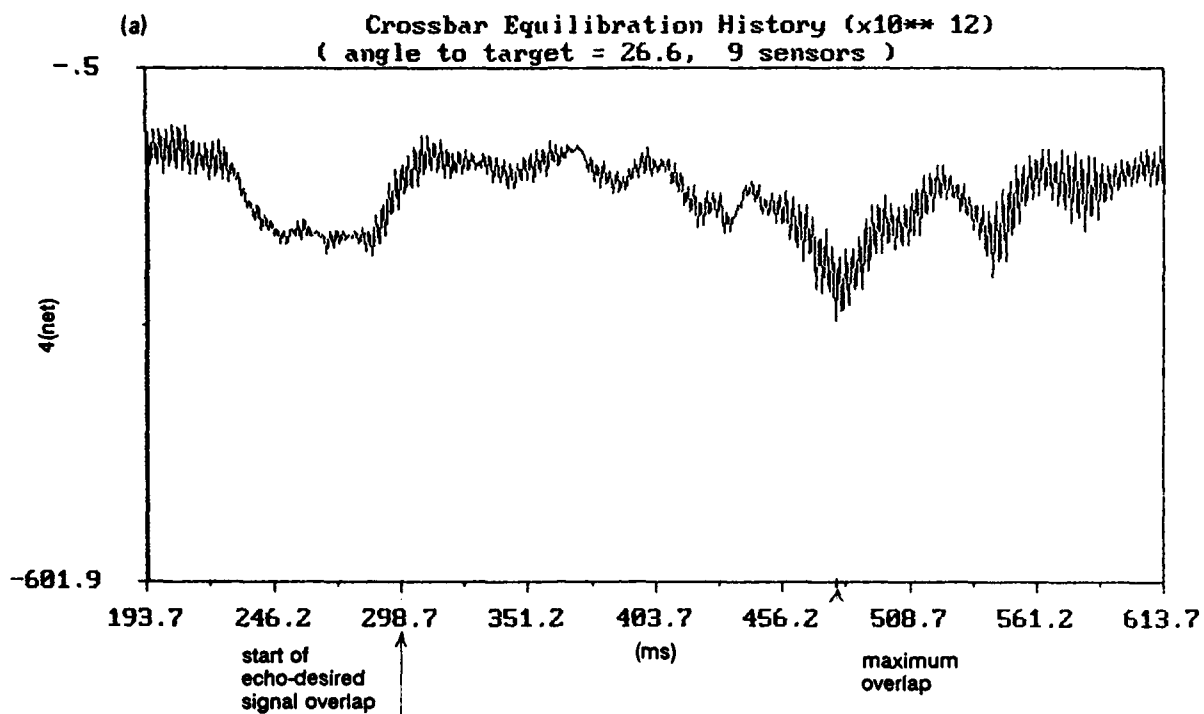


Figure 21. Crossbar network energy history for case: point target, SIR = -15 dB, speed = 0 knot.

(a)



(b)



Figure 22. Snapshots of evolving/adapting beams on polar scale for: (a) before target echo return, (b) after target echo return. Beam is yellow because the SIR is -15 dB and the energy does not go as low as for the case, SIR = 0 dB. Target is at 26 degrees.

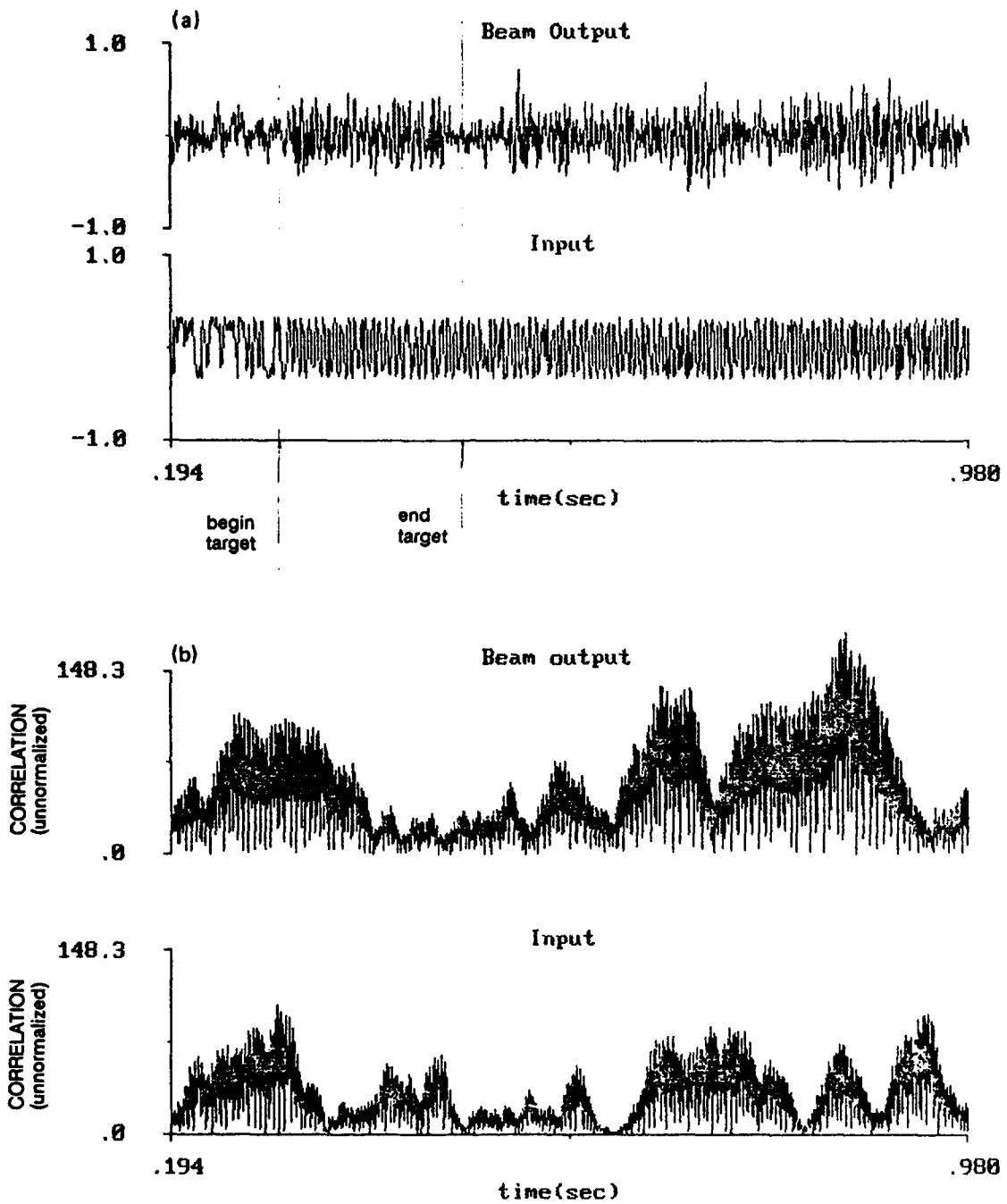


Figure 23. (a) Beam output and input stream for channel 1.
 (b) Matched-filter/cross-correlation values.

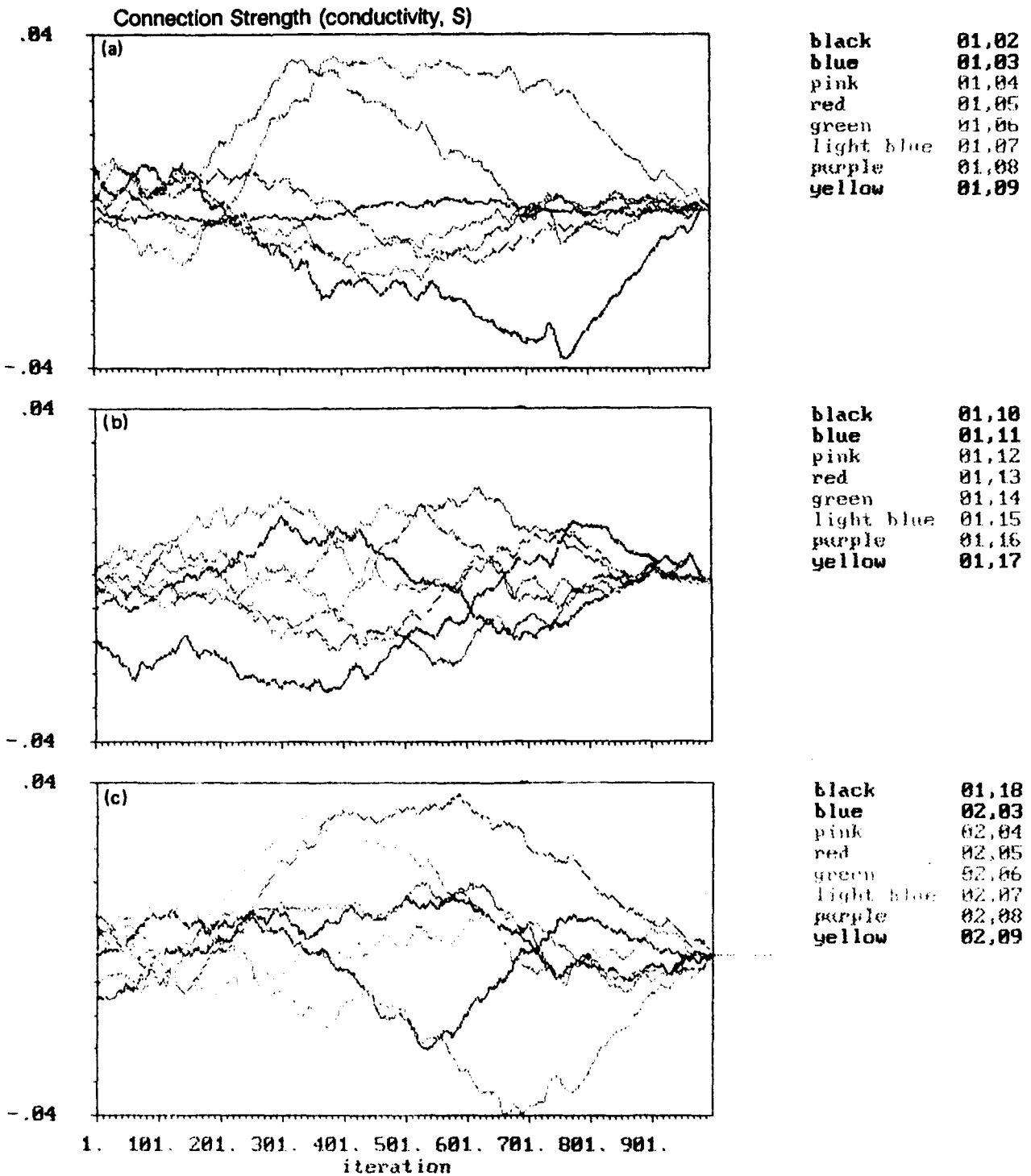


Figure 24. Connectivity histories for the case: point target, SIR = -15 dB, speed = 0 knot. (iteration = 0.8 ms).

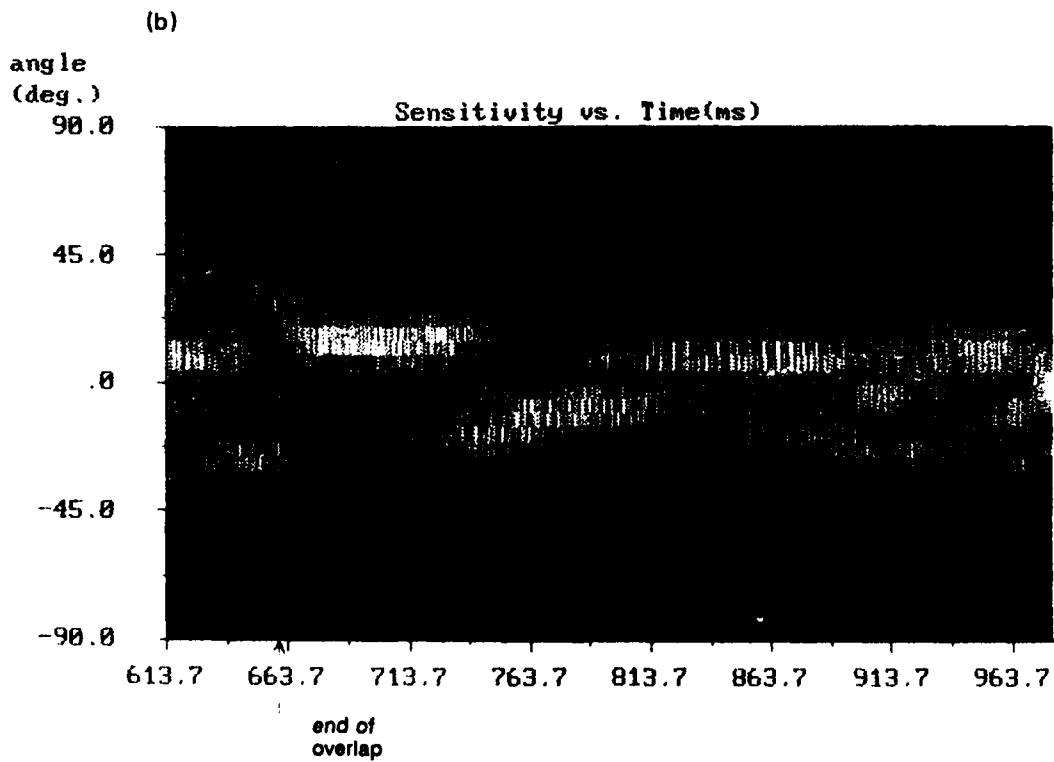
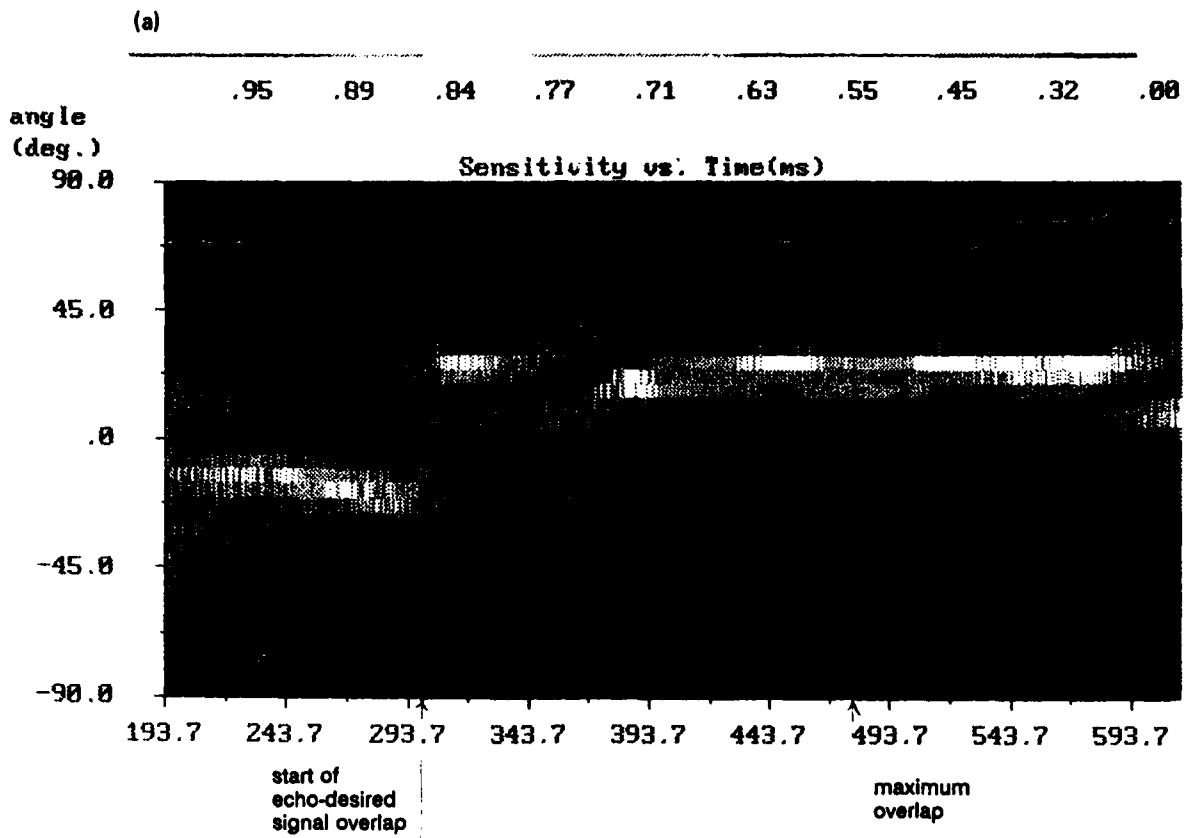


Figure 25. Sensitivity history for case: distributed target, SIR = 0 dB, speed = 0 knot.

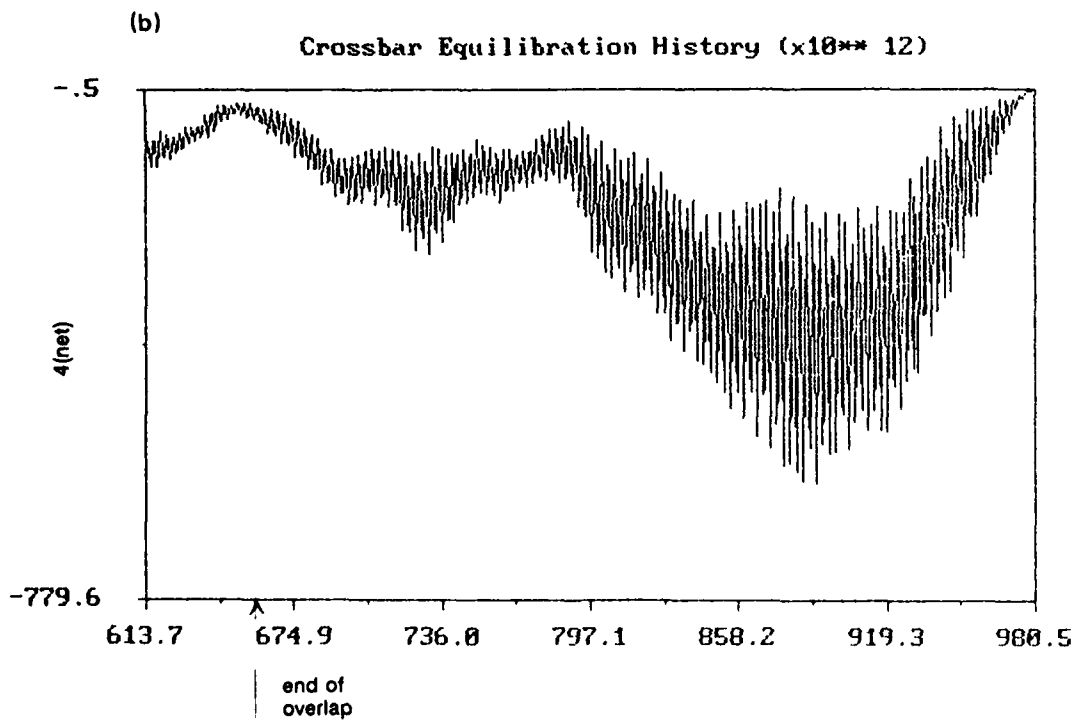
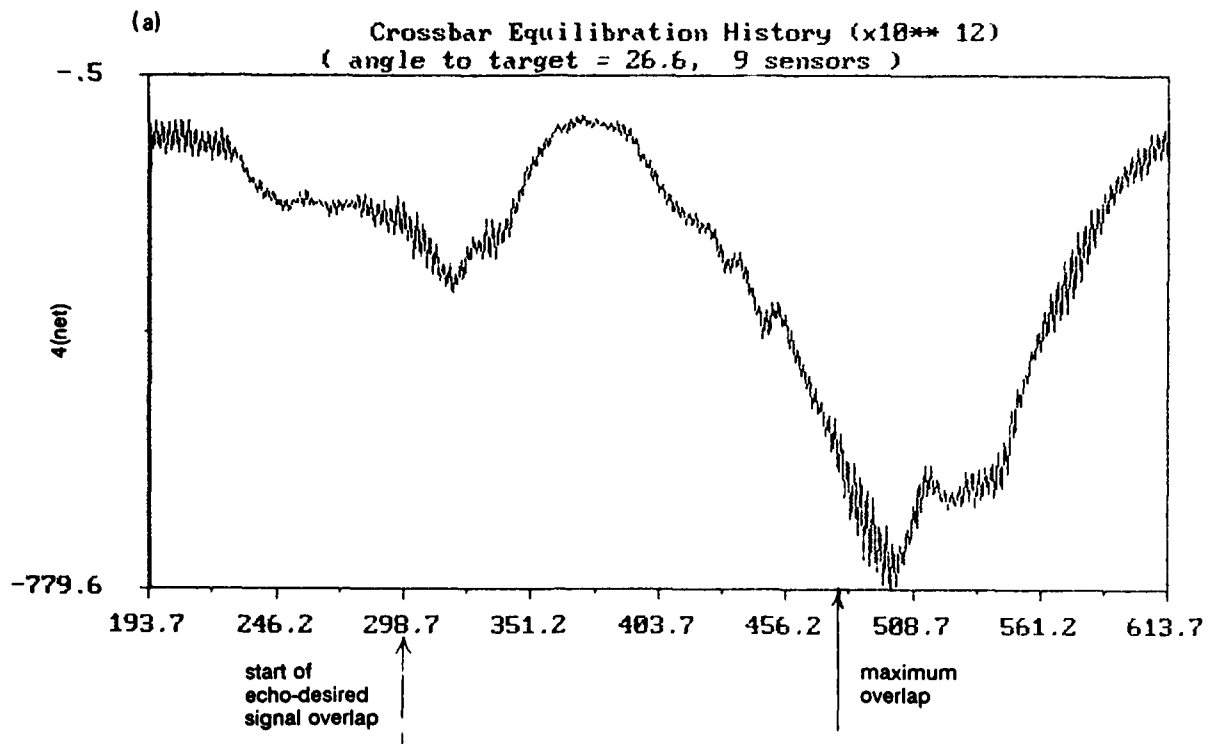


Figure 26. Crossbar network energy history for case: distributed target, SIR = 0 dB, speed = 0 knot.

(a)



(b)



Figure 27. Snapshots of evolving/adapting beam on a polar scale for case: distributed target,
SIR = 0 dB, speed = 0 knot.

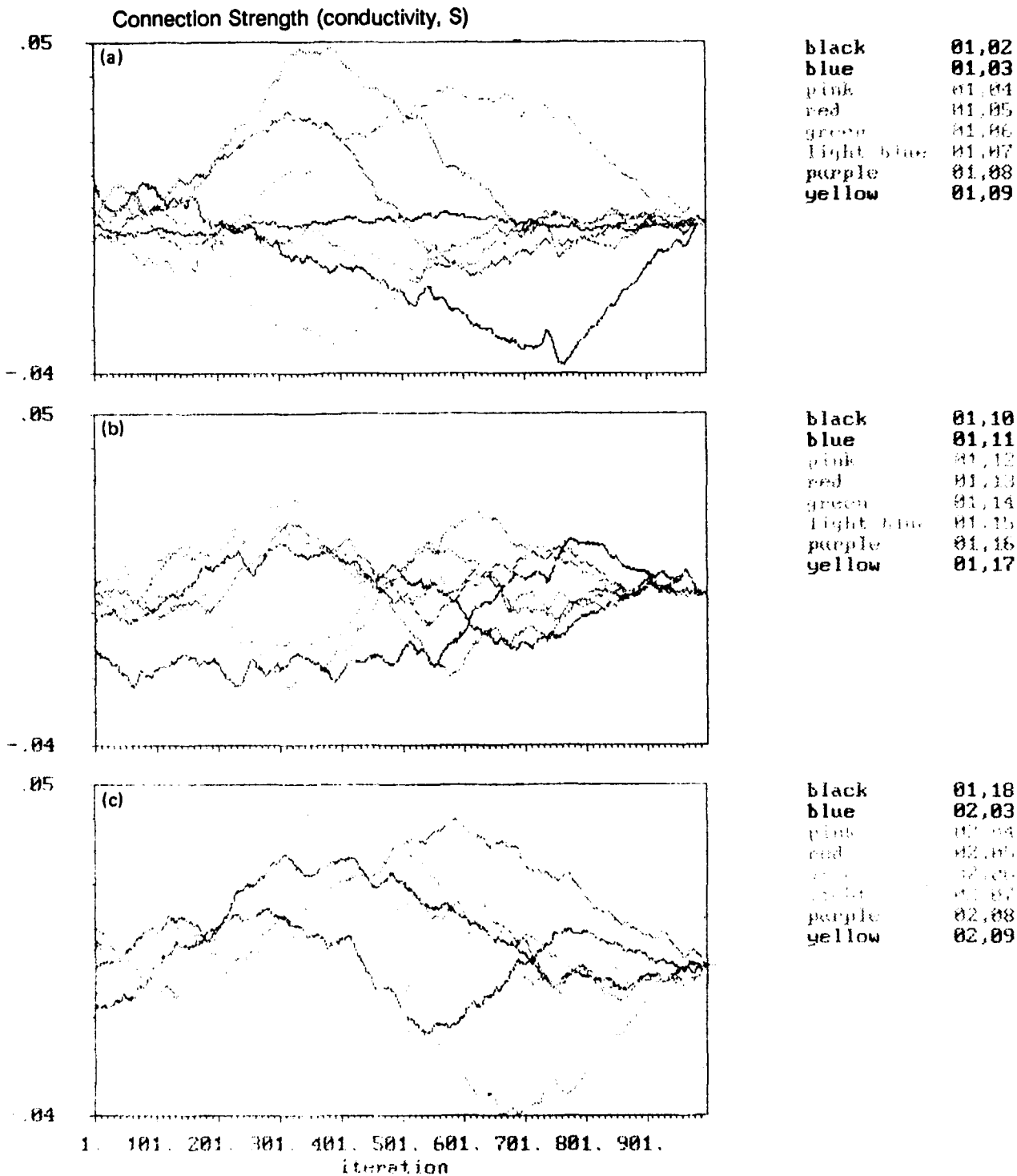


Figure 28. Connection strength histories for case: distributed target, SIR = 0 dB, speed = 0 knot. (iteration = 0.8 ms).

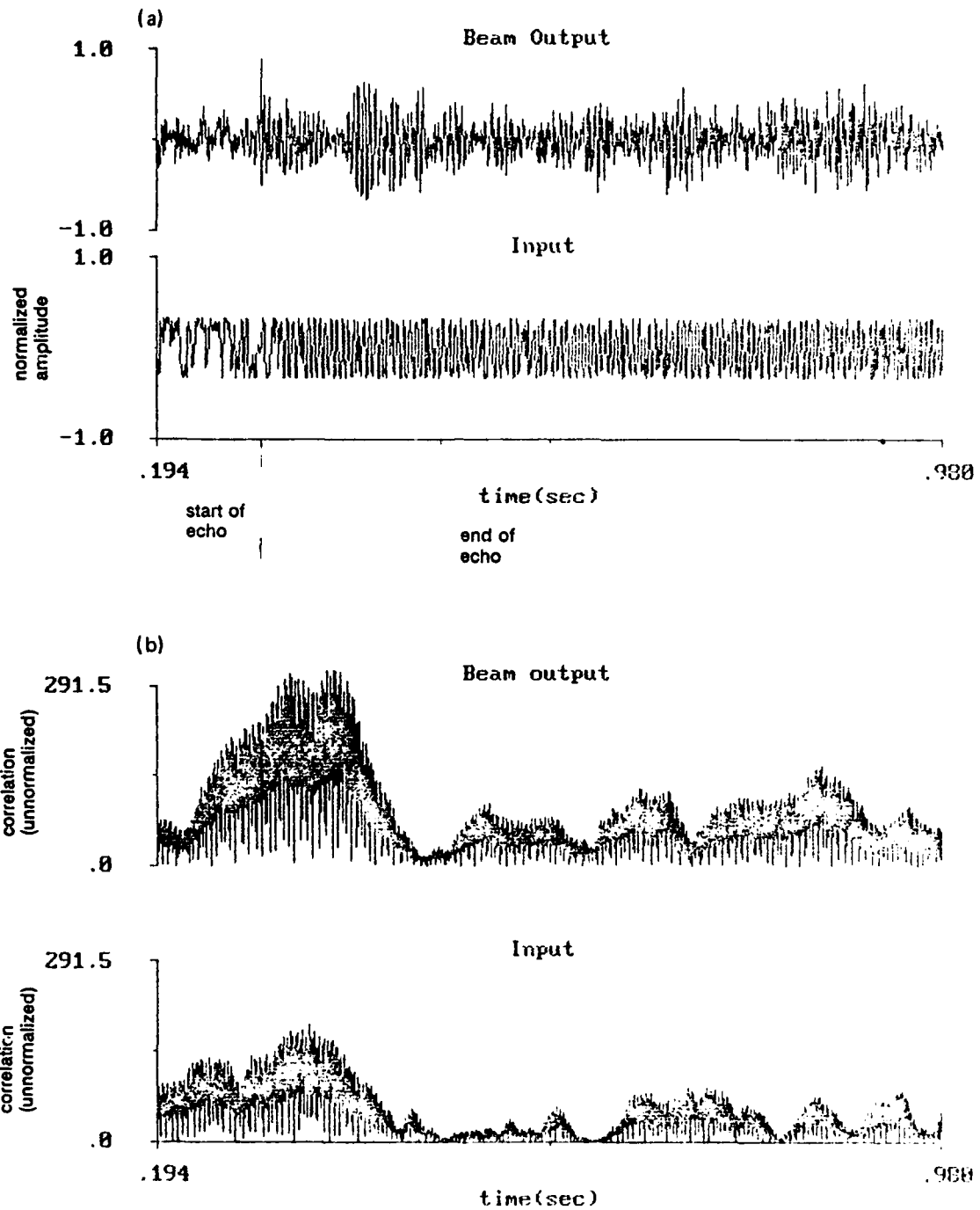


Figure 29. (a) Beam output and input stream for channel 1. (b) Matched-filter cross-correlation values case: distributed target, SIR = 0 dB, speed = 0 knot.

7. GENERAL CONSIDERATIONS AND CAPABILITIES

7.1 OVERVIEW

The investigation covered by this report emphasizes the crossbar method of beamforming. This method essentially effects control over a crossbar network in order to optimize the beam output in the least squares sense. This causes experiential adaption to occur, i.e., there is no supervised learning necessary, the beamformer adapts "on-the-fly", continually looking for the "desired signal" to appear within the inputs.

The parameter estimator, described in the section 7.2.4, is combined with the signal-processing technique of using phase-shifted input to allow the network to operate on phase. It can be shown that it is not necessary to use quadrature pairs in order to achieve the adaptive phase shifting of inputs, but it is more efficient to do so.

It has been suggested that a differentiator be used to effect the phase shift. This method would account somewhat for the bandwidth of the signals, shifting the spectral components by 90 degrees. Another way to increase the bandwidth of the beamformer is to filter the input into separate bands. This could be used in combination with the differentiation.

In the previous report on the neurobeamformer¹⁹ a second method was reported, called the bivector beamformer.* This method introduced the modified Kohonen learning rule and competitive learning. It is now realized that some of the characteristics of this method can be realized within a networked crossbar beamformer configuration. They can be made to compete, for instance, which would allow them to track several objects simultaneously as mentioned below in "Maneuvering among obstacles or landmarks".

The bivector beamforming method is still of interest to us because of its ability to search for statistically "stable" phase patterns within the signal space, not requiring a desired signal to be fed in. Sometimes one does not know what the mission-relevant signal is going to be, so the most effective approach is to lock on to relatively persistent returns and noise-cancel them in order to get as clean a signal as possible for comparison with a database of known signals.

7.2 APPLICATIONS

Some brief examples follow.

7.2.1 Guiding Weapons to their Mission Targets

Guiding weapons to their mission targets is an important military application. The function of the neurobeamformer in this case, is to find a signal which is characteristic to the target from within noise and interference and enhance the signal relative to noise and interference.

The target signal is detected by the special processing technique already mentioned and outlined in detail in a later section. The circuit increases target SIR by directing a beam in the correct direction. Since the sensitivity to other directions is reduced, noise and interference are reduced. Thus, the candidate target signal is more easily recognized/classified.

*NOSC Technical Notes (TNs) are working documents and do not represent an official policy statement of the Naval Ocean Systems Center. For further information, contact the author.

Interference rejection can be further enhanced and cancellation introduced by incorporating multiple neurobeamformers into a network. This allows beam-to-beam interaction which increases the ability to resolve spatial sectors and cancels sidelobes, thereby enhancing interference cancellation with respect to what can be achieved with a single beam. It also has additional features, which are discussed in a previous section on the neuroprocessor.

7.2.2 Maneuvering Among Obstacles or Landmarks

For an autonomous vehicle maneuvering along the ocean bottom, one would like for it to avoid obstacles and keep track of its location as it moves along. It can do this by pinging upon its surroundings and tracking individual objects.

One step in the process of tracking the objects is to use an adaptive beamformer. Although the echoes received from objects at nearly equal ranges are temporally overlapped, the beamformer would partition the individual object returns into separate channels, and a track kept for each one. As the platform moves, the beams adapt to keep the objects on main response axes. To achieve this effect, a network of beamformers are made competitive.

7.2.3 Image Processing

In sensor systems which detect electromagnetic radiation in the visible range, the sensor outputs are, loosely speaking, representative of average intensities. The frequencies are very high, and the waveform is not analyzed in detail.

However, if we take a raster scan of an image as in video applications, then the individual pixel intensities, taken in sequence, form temporal patterns. We can then utilize the neurobeamformer's capability as a temporal pattern recognizer. These raster scan patterns can be fed into the neurobeamformer as separate channels while scan lines representing the object of interest (OI) are fed in also. The action of the network is to recognize the desired pattern from within the image scan and select the proper scan lines which contain the OI.

If orthogonal scans are simultaneously processed, then the selected rows and columns indicate the position of the OI within the image. If a lens has focused the subject image onto the sensor, then the position of the OI within the image indicates the direction to the OI in the reference frame of the lens-sensor system.

The specific application could be looking for a particular word or phrase in a page of text, finding a flying object in the visual field, or controlling the proper placement of a part on an assembly line.

7.2.4 General Least Square Parameter Estimation

At the heart of the subject devices is the technique for controlling the crossbar network in order to form an experientially adaptive, least square parameter estimator. This means that, given a set of basis functions and incoming data, the device finds the correct weights to apply to the basis functions to form an estimate of the incoming data with minimum mean square error.

An example application of this general capability is to use it to do a Discrete Fourier Transform (DFT). This is achieved by using sinusoids as the basis functions, i.e., $\sin w_1 t$, $\cos w_1 t$, $\sin w_2 t$, $\cos w_2 t$, . . . etc. Use of more complex basis functions, for the purpose of target recognition, has been explored by Altes.²⁰

8. REFERENCES

1. Bucciarelli, T., M. Esposito, A. Farina, G. Losquadro. 1982. "The Gram-Schmidt Sidelobe Canceller," *International Conference Radar-82*. Publ. IEE, London England, pp. 486-490.
2. Hodgkiss, W., and D. Alexandrou. March 1986. "An Adaptive Algorithm for Array Processing", *IEEE Transactions on Antennas and Propagation*, vol. AP-34, no. 3.
3. Davis, R.C., L.E. Brennan, and L.S. Reed. March 1976. "Angle Estimation With Adaptive Arrays in External Noise Fields", *IEEE Transactions on Aerospace and Electronic Systems*, vol. AES-12, no. 2.
4. Sejnowski, T., C. Koch, and P. Churchland. September 1988. "Computational Neuroscience", *Science*, vol. 241, p. 1300.
5. White, G., W.B. Levy, and O. Steward. April 1988. "Evidence that Associative Interactions Between Synapses During the Induction of Long-Term Potentiation Occur Within Local Dendritic Domains," *Proc. Nat. Acad. Sci., USA*, vol. 85.
6. Stanton, P.K., J. Jester, S. Chattarji, and T.J. Sejnowski. "Storage of Covariance by the Selective Long-Term Potentiation and Depression of Synaptic Strengths in the Hippocampus", Department of Biophysics, Johns Hopkins University.
7. Hopfield, J. and D. Tank. 1985. "Neural Computation of Decisions in Optimization Problems," *Biol. Cybern.*, 52, pp. 141-152.
8. Templeman, J.N. 1988. "Race Networks: A Theory of Competitive Recognition Networks Based on the Rate of Reactivation of Neurons in Cortical Columns", *Proceedings of the Second ICNN*, IEEE.
9. Livingstone, M., and D. Hubel. May 1988. "Segregation of Form, Color, Movement, and Depth: Anatomy, Physiology, and Perception," *Science*, vol. 240.
10. Geisler, C.D. 1988. "Representation of Speech Sounds in the Auditory Nerve", *J. of Phonetics*, 16.
11. Greenberg, S. 1988. "The Ear as a Speech Analyzer," *J. of Phonetics*, 16.
12. Lindemann, W. December 1986. "Extension of a Binaural Cross-Correlation Model by a Contralateral Inhibition. I. Simulation of Lateralization for Stationary Signals," *JASA*, 80.
13. Lindemann, W. December 1986. "Extension of a Binaural Cross-Correlation Model by Contralateral Inhibition. II. The Law of the First Wave Front," *JASA*, 80.
14. Shamma, S.A. November 1985. "Speech Processing in the Auditory System I: The Representation of Speech Sounds in the Responses of the Auditory Nerve," *JASA*, 78.
15. Colburn, H.S., and J.S. Latimer. July 1978. "Theory of Binaural Interaction Based on Auditory Nerve Data. III. Joint Dependence on Interaural Time and Amplitude Differences in Discrimination and Detection," *JASA*, 64.
16. Stern, R.M., and H.S. Colburn. July 1978. "Theory of Binaural Interaction Based on Auditory-Nerve Data. IV. A Model for Subjective Lateral Position," *JASA*, 64.
17. Deng, L., C.D. Geisler and S. Greenberg. 1988. "A Composite Model of the Auditory Periphery for the Processing of Speech," *J. of Phonetics*, 16.
18. Shamma, S.A. November 1985. "Speech Processing in the Auditory System II: Lateral Inhibition and the Central Processing of Speech Evoked Activity in the Auditory Nerve," *JASA*, 78(5).

19. Speidel, S.L. July 1988. *Neurobeamformer: Adaptive Beamforming via Neural Networks*, NOSC TN1540.
20. Altes, R.A., 1980. "Models for Echolocation," *Animal Sonar Systems*, Busnel and Fish, Eds., Plenum Press, New York.

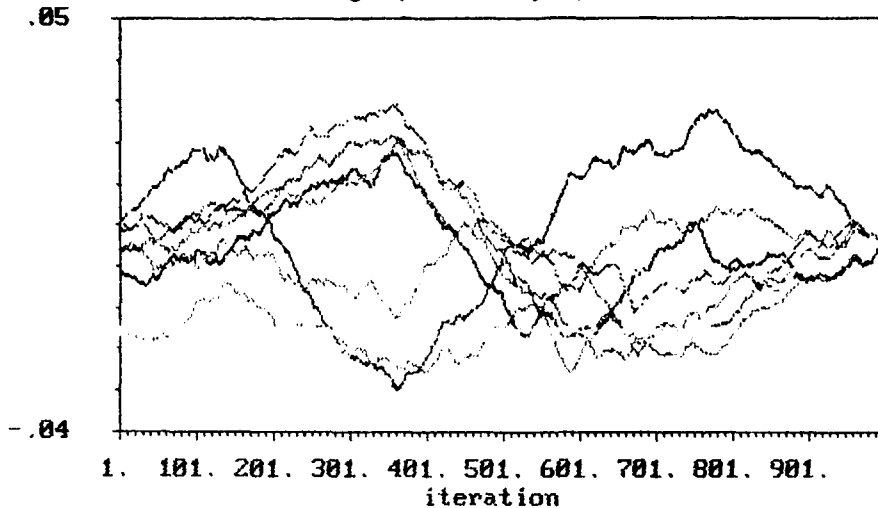
9. GLOSSARY

amps	amperes
ANN	artificial neural network
ANZA	Zenith 386 machine with Hecht-Nielson 68020-based coprocessor board
APL/PS	Applied Physics Laboratory, Penn State Univ.
ASW	antisubmarine warfare
dB	decibels
deg	degrees
DFT	Discrete Fourier Transform
Freq	frequency
Hz	hertz
kcps	kilocycles per second (now kHz)
kHz	kilohertz
LTP	long-term potentiation
MMSE	minimum mean square error
MPL	Marine Physical Laboratory
ms	millisecond
OI	object of interest
PE	processing elements
S	Siemens
sec	second
SEG	standard echo generator
SIR	signal-to-interference ratio
TSSP	target strength standardization program
VLSI	very large scale integration

**APPENDIX A—
Connection Strength Plots
Point Target, SIR = 0 dB
(Iteration \approx 0.8 ms)**

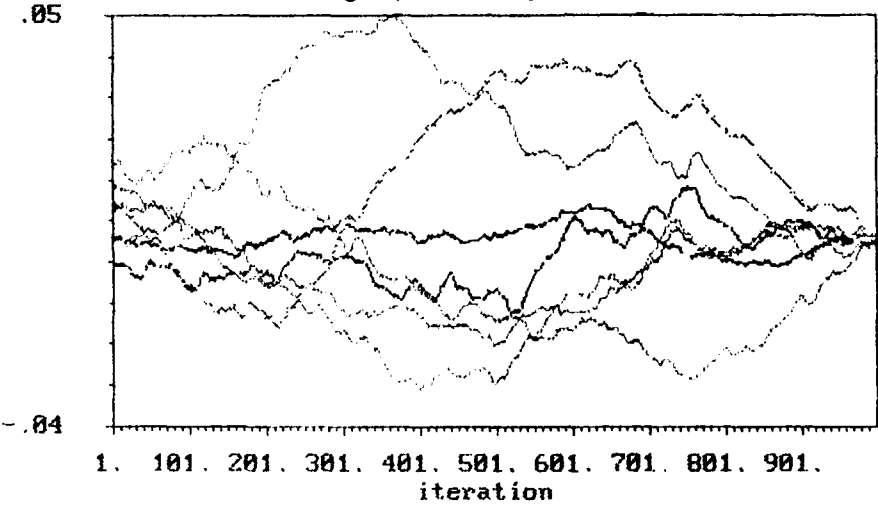
A-1 / A-2

Connection Strength (conductivity, S)



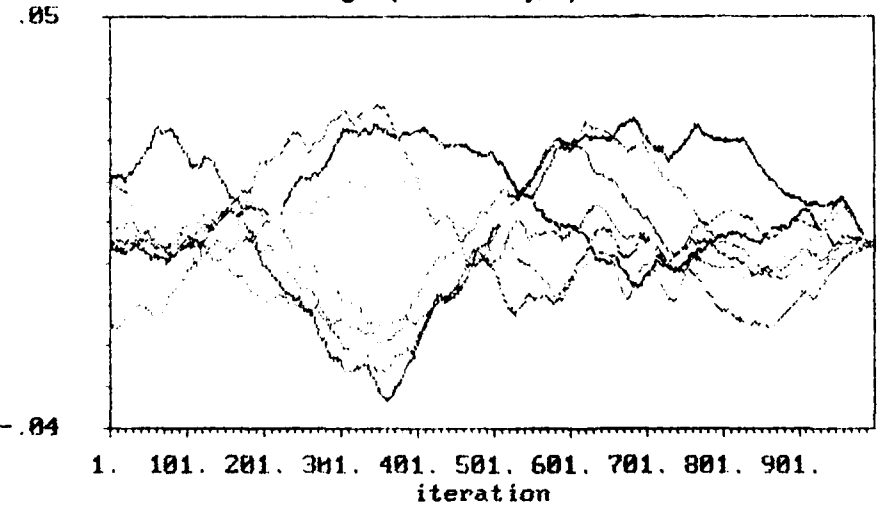
black	02,10
blue	02,11
pink	02,12
red	02,13
green	02,14
light blue	02,15
purple	02,16
yellow	02,17

Connection Strength (conductivity, S)

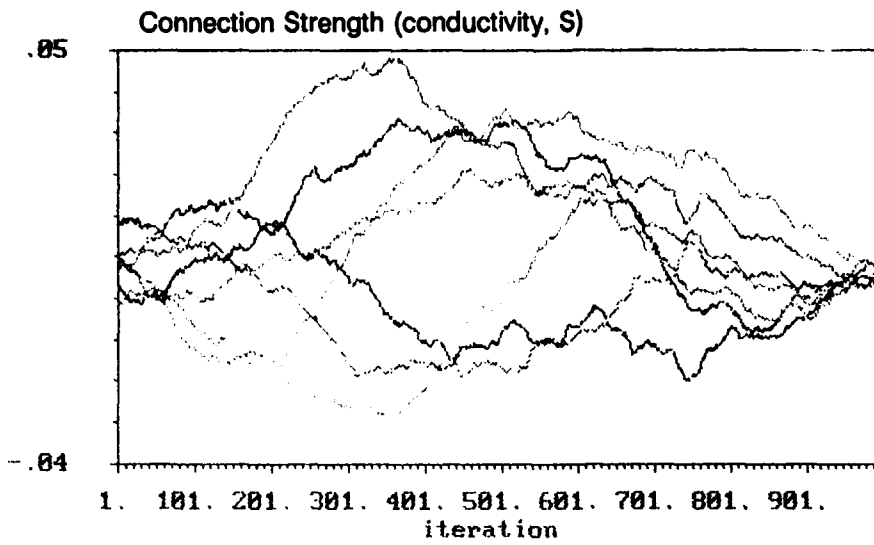


black	02,18
blue	03,04
pink	03,05
red	03,06
green	03,07
light blue	03,08
purple	03,09
yellow	03,10

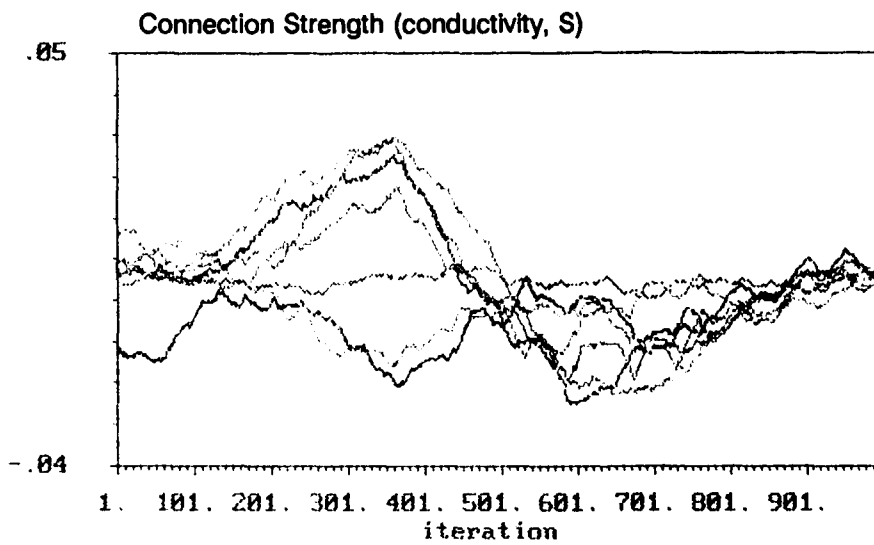
Connection Strength (conductivity, S)



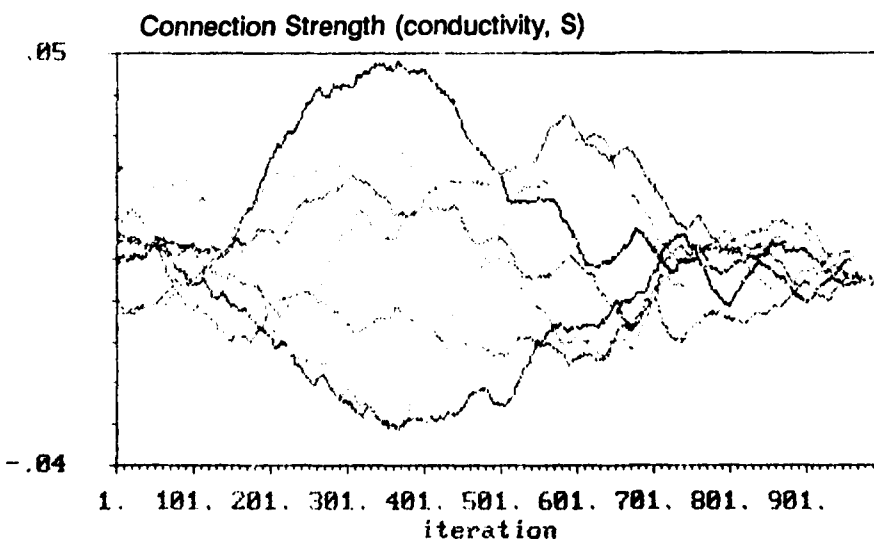
black	03,11
blue	03,12
pink	03,13
red	03,14
green	03,15
light blue	03,16
purple	03,17
yellow	03,18



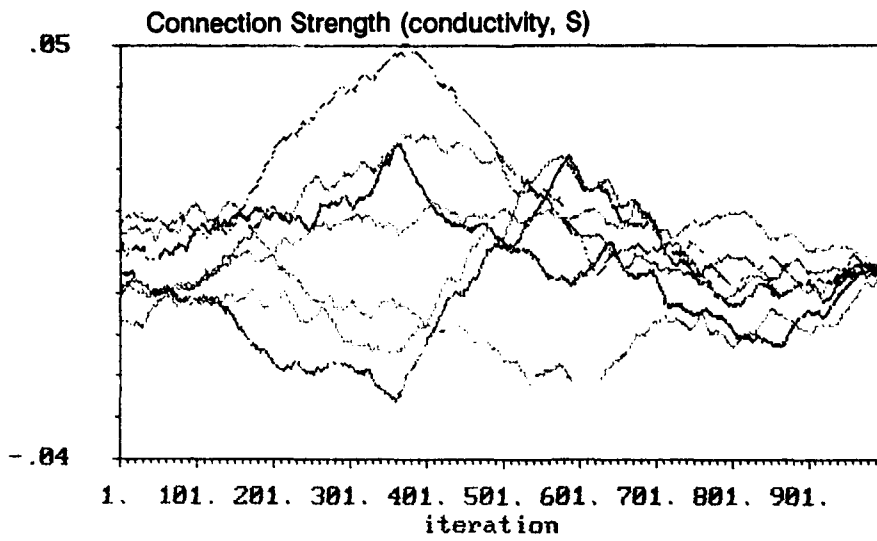
black	04,05
blue	04,06
pink	04,07
red	04,08
green	04,09
light blue	04,10
purple	04,11
yellow	04,12



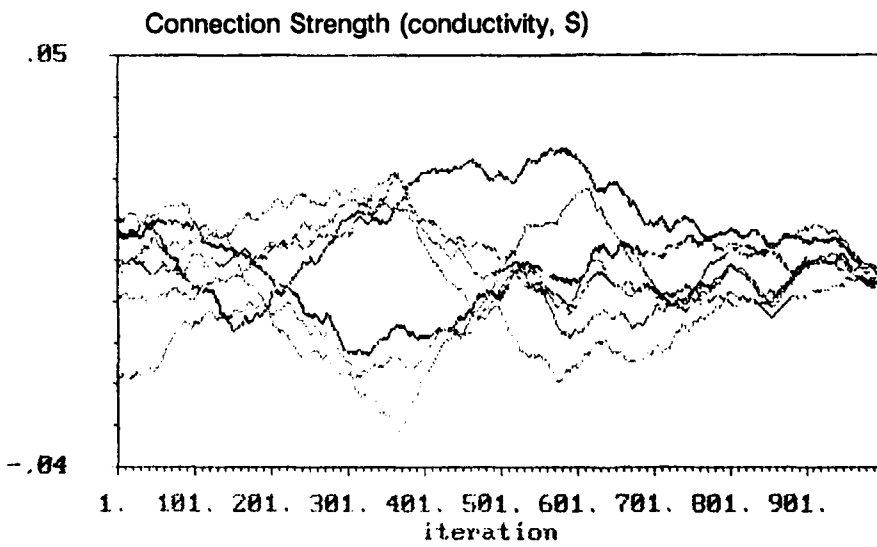
black	04,13
blue	04,14
pink	04,15
red	04,16
green	04,17
light blue	04,18
purple	05,06
yellow	05,07



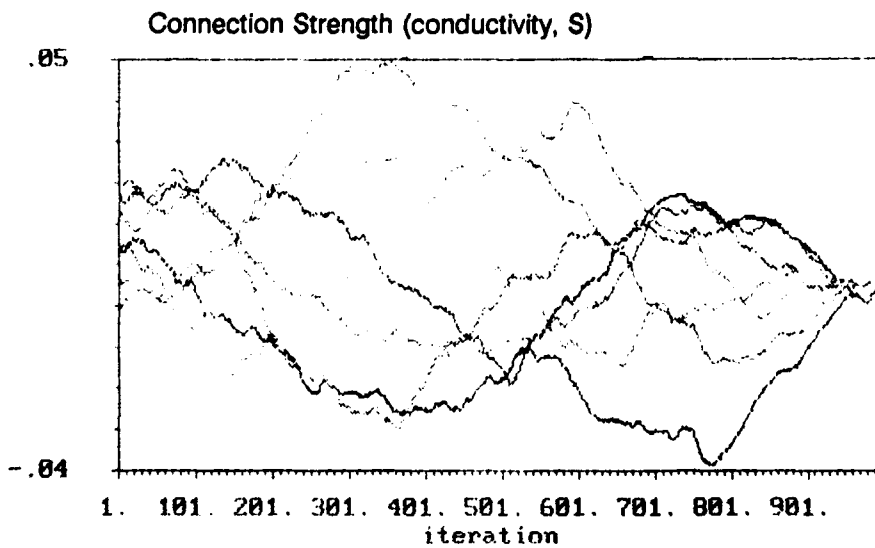
black	05,08
blue	05,09
pink	05,10
red	05,11
green	05,12
light blue	05,13
purple	05,14
yellow	05,15



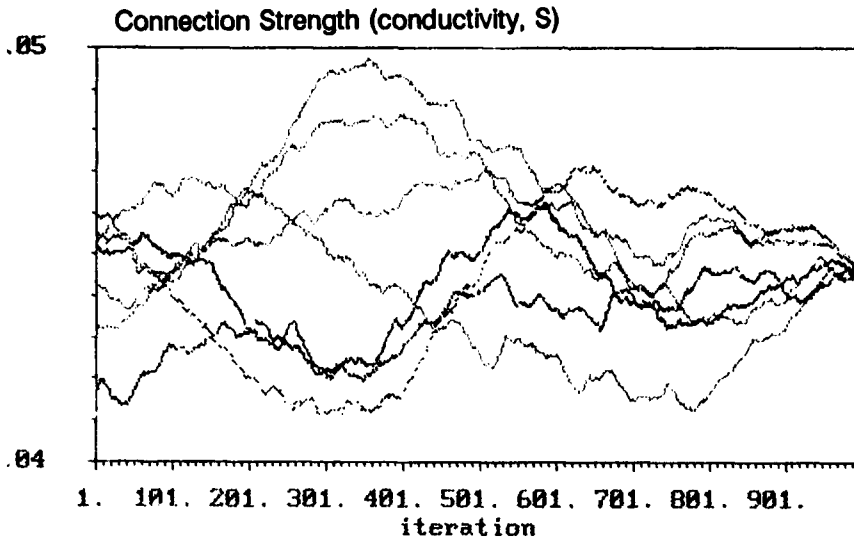
black	05,16
blue	05,17
pink	05,18
red	06,07
green	06,08
light blue	06,09
purple	06,10
yellow	06,11



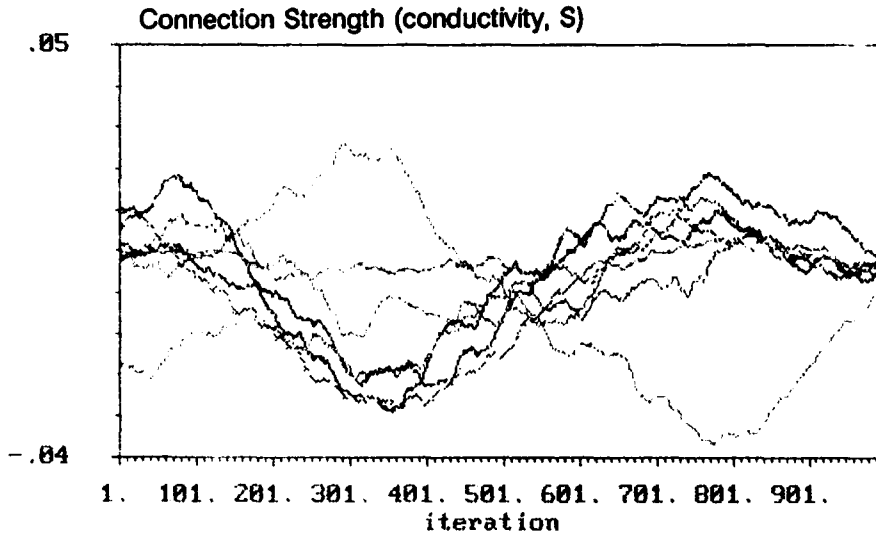
black	06,12
blue	06,13
pink	06,14
red	06,15
green	06,16
light blue	06,17
purple	06,18
yellow	07,08



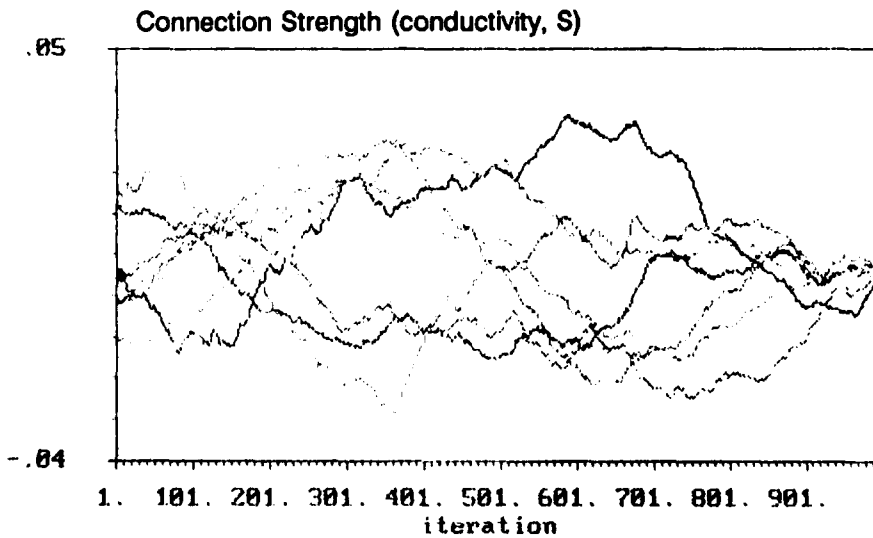
black	07,09
blue	07,10
pink	07,11
red	07,12
green	07,13
light blue	07,14
purple	07,15
yellow	07,16



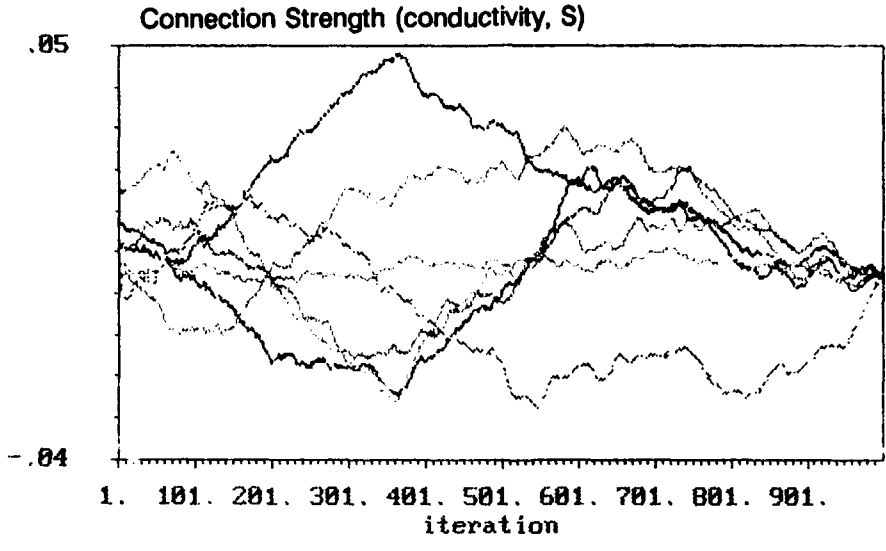
black	07,17
blue	07,18
pink	08,09
red	08,10
green	08,11
light blue	08,12
purple	08,13
yellow	08,14



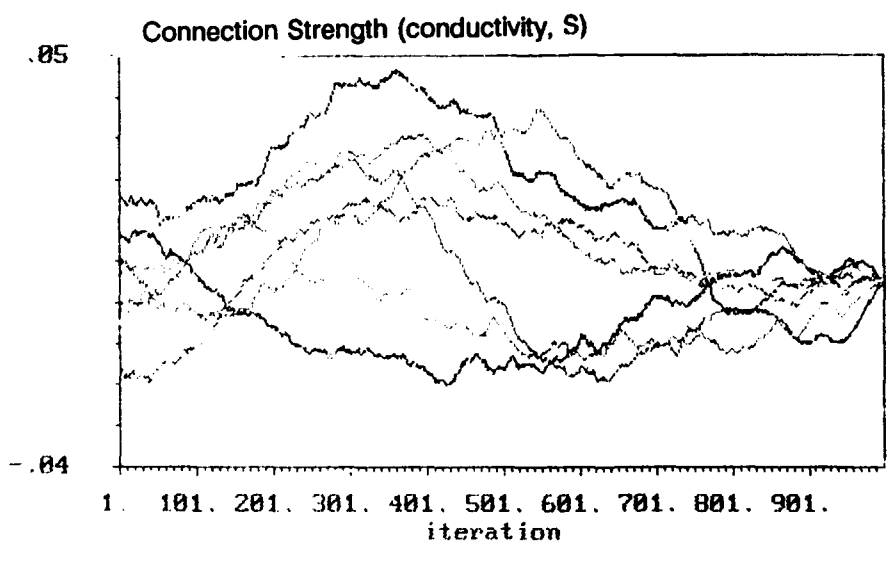
black	08,15
blue	08,16
pink	08,17
red	08,18
green	09,10
light blue	09,11
purple	09,12
yellow	09,13



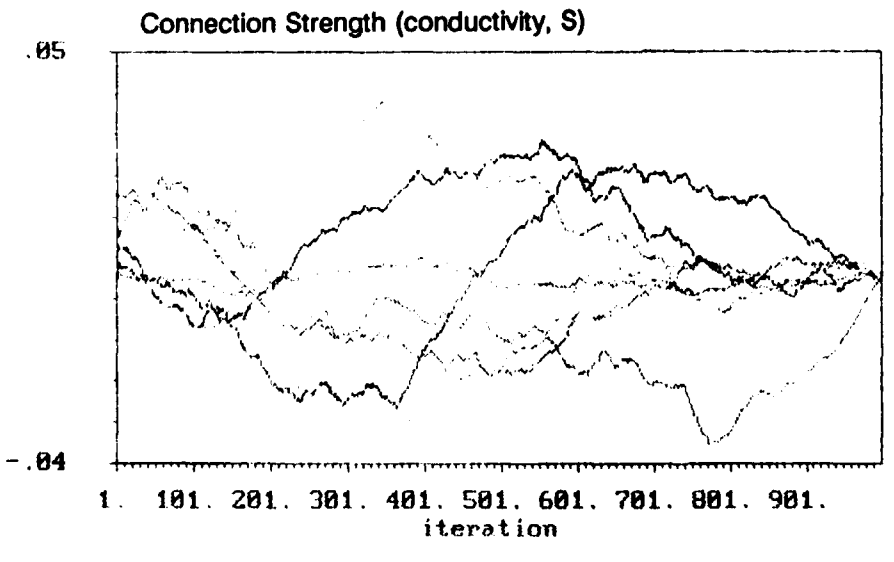
black	09,14
blue	09,15
pink	09,16
red	09,17
green	09,18
light blue	10,11
purple	10,12
yellow	10,13



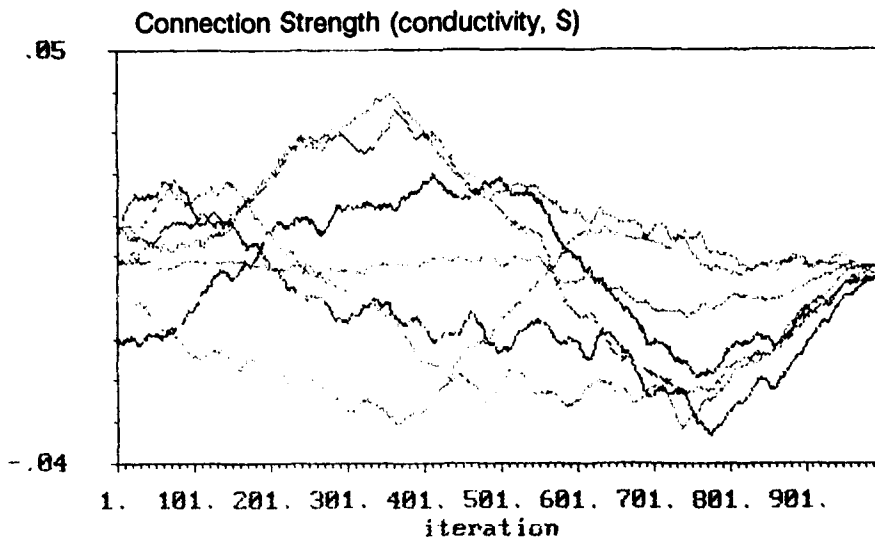
black	10,14
blue	10,15
pink	10,16
red	10,17
green	10,18
light blue	11,12
purple	11,13
yellow	11,14



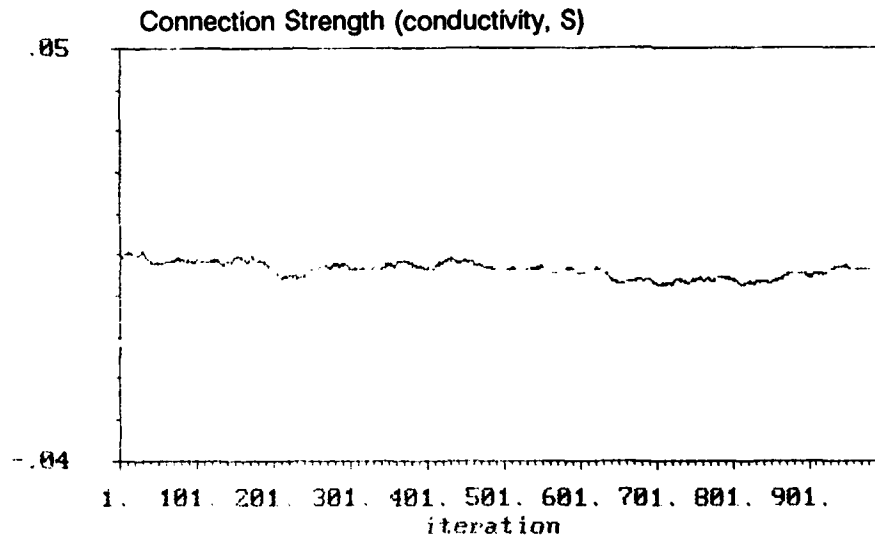
black	11,15
blue	11,16
pink	11,17
red	11,18
green	12,13
light blue	12,14
purple	12,15
yellow	12,16



black	12,17
blue	12,18
pink	13,14
red	13,15
green	13,16
light blue	13,17
purple	13,18
yellow	14,15



black	14,16
blue	14,17
pink	14,18
red	15,16
green	15,17
light blue	15,18
purple	16,17
yellow	16,18



black	17,18
blue	01,01
pink	01,01
red	01,01
green	01,01
light blue	01,01
purple	01,01
yellow	01,01